Replies to Referee #1

Projected increases in magnitude and socioeconomic exposure of global droughts in 1.5 °C and 2 °C warmer climates

Lei Gu, Jie Chen, Jiabo Yin, Sylvia C. Sullivan, Hui-Min Wang, Shenglian Guo, Liping Zhang, and Jong-Suk Kim

We thank the anonymous referee for the constructive comments and queries. We have provided detailed responses to each comment below and will revise the manuscript accordingly. For clarity, comments are given in *italics*, and our responses are given in plain text.

Authors' responses

Legend

Reviewer's comments

Authors' responses

In this manuscript, the authors used the SPEI and run theory to define drought events, analyzed the variations of drought severity and duration by joint return period based on copula function and highlighted changes in exposures of population and GDP to global drought under three RCP scenarios (corresponding to three SSPs) at 1.5°C and 2°C warming targets. The idea of studying the socioeconomic exposures to global drought is meaningful for countries concerned to understand and mitigate potential drought risks in the future. Generally, the manuscript is well organized with clear logic, before I recommend it for publication, major improvements are still needed.

We appreciate the reviewer's positive evaluation and professional comments on our manuscript. Please find our point-by-point responses below.

1. When discussing the increase in the magnitude of global drought, the severity and duration of drought are both considered using a copula function and the drought is defined using SPEI< -0.5 and run theory, the methods are all good. As in table 2 indicates, SPEI <-0.5 incorporates three different levels of drought from mild, moderate

to extreme drought. The authors used copula function to consider both the severity and duration, however, the severity of drought retrieved from the run theory may not reveal the distribution of different levels of drought? Although authors discussed the threshold of 0.8 to confirm relevant results, whether the selection of this threshold may further influence the results of socioeconomic exposures to droughts is worth thinking.

Reply: Thanks for this comment. We agree with the reviewer that the selection of threshold needs to be further clarified. Please find it as follows:

In the run theory, once the threshold (e.g., -0.5) is determined, drought events with different severity magnitudes are identified and constitute a sample for the selected time period. This sample contains different magnitudes in severity and different lengths in the duration, therefore, characterizes the distribution of different levels of drought (ranging from the mild, moderate to extreme conditions). In addition, the gamma distribution is applied to fit the distribution of different magnitudes of drought severity. To further confirm our results regarding drought risks under different levels of global warming, the threshold of -0.8 is also utilized, and the results derived from this threshold are similar to those from -0.5. Since the calculation of socioeconomic exposures to droughts is based on the variations of 50-year drought risk, similar changes in the drought risk will lead to analogical socioeconomic exposures. In other words, under a certain RCP scenario and for a certain warming level, drought risk changes determine the socio-economic exposures when employing the same dynamic population (and GDP) pathways. As a reference, we also analyze the socioeconomic exposures in the case when -0.8 is used as the threshold (Figs. R1-2). Compared with the results of the -0.5 threshold (Figs. 9-10), the overall characteristics of the drought exposures are mostly the same.

Furthermore, we also derive changes in drought risks for the 20-year or 100-year drought events to explore risk variations caused by different extents of drought (Figs. R3-4). Results shows that although the magnitudes of changes are different, they present quite similar spatial patterns.

These points have been added to the Discussion section of the revised manuscript (Page 20, Lines 26-29; Page 21, Lines 1-6), and Figs. R1-4 have been added in the supplementary (Fig. S5-8).

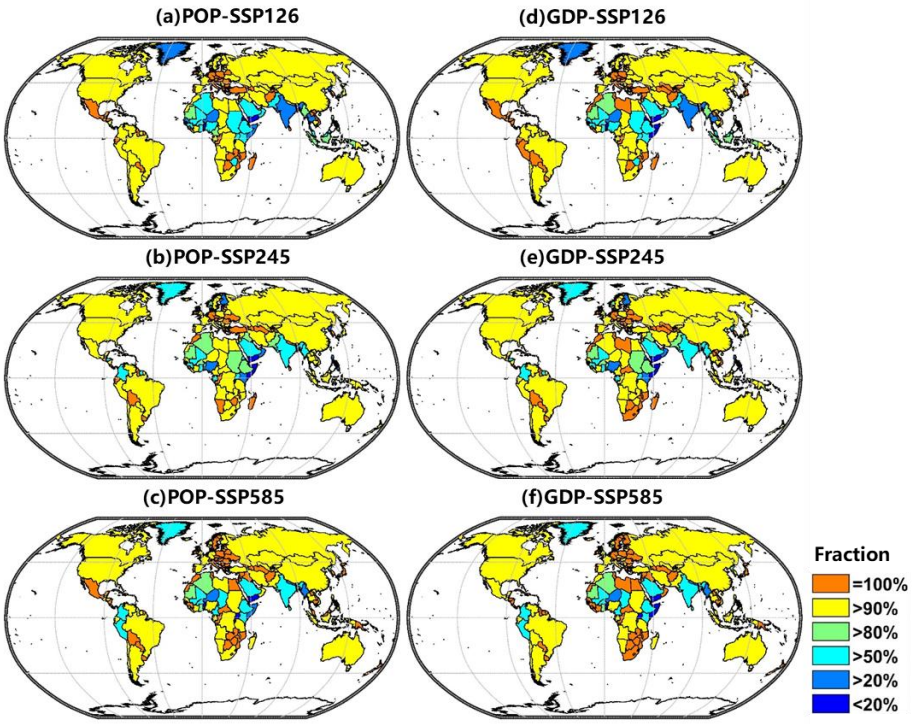

Figure R1 National population and GDP fraction exposing to more frequent severe droughts under the 1.5°C warming level (based on the -0.8 threshold)

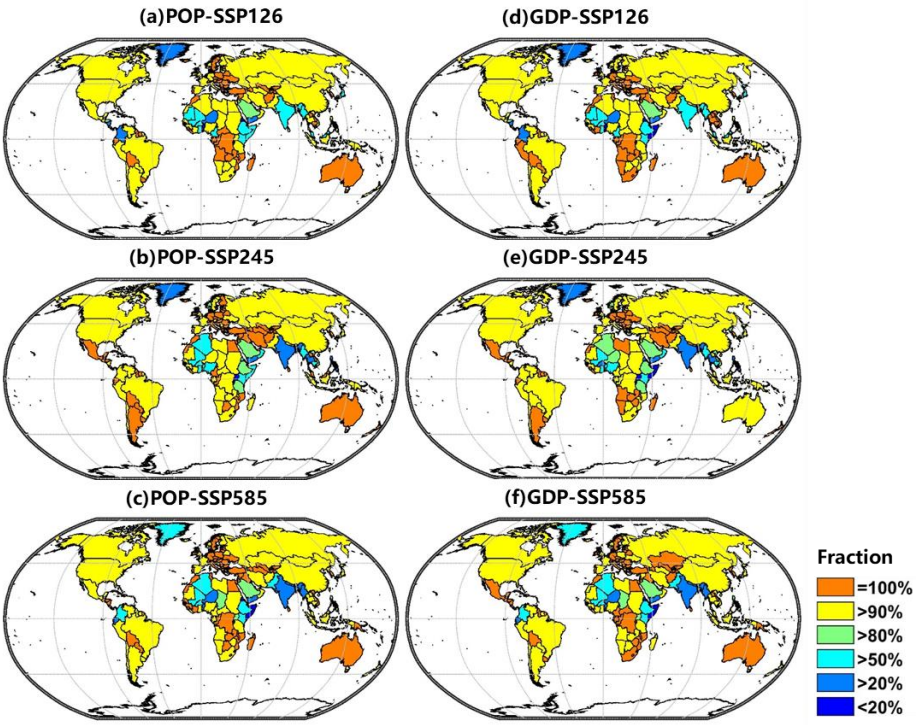

Figure R2 National population and GDP fraction exposing to more frequent severe droughts under the 2.0°C warming level (based on the -0.8 threshold)

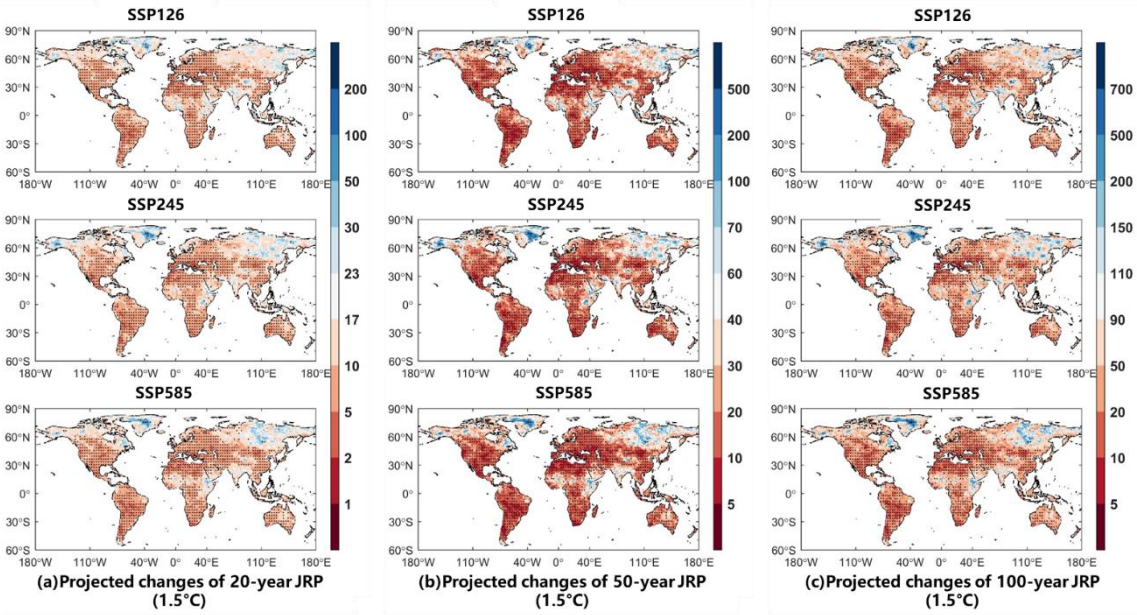

Figure R3 Projected changes of 20-, 50-, and 100-year joint return period of droughts under the 1.5°C warming level.

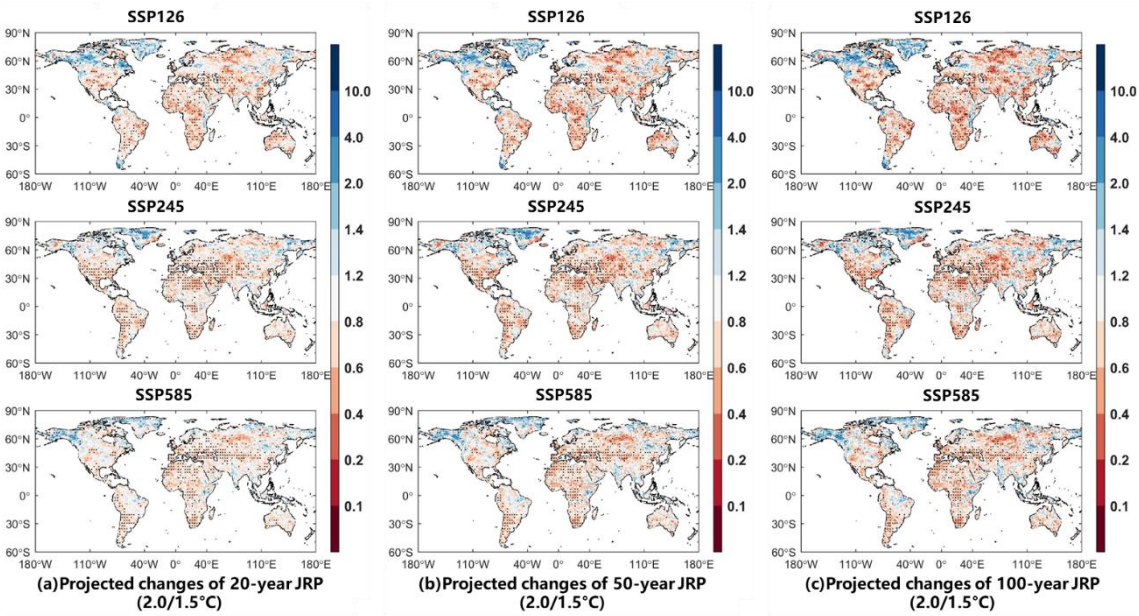

Figure R4 Projected changes of 20-, 50-, and 100-year joint return period of droughts between the 1.5°C and 2.0°C warming level.

2. When calculating SPEI with Penman-Monteith-based PET, the term ($0.34u_2$) in the equation is finally obtained through the ratio rs/ra and represents the suggested reference crop surface (assuming a standard plant height of 0.12 m, affixed surface

resistance of 70 sm-1 and an albedo of 0.23). However, considering a distinct vegetation response to elevated CO_2 as simulated in the fully coupled climate models, it is important to point out that some of the assumptions that underlie the computation of PET (and thus SPEI) are incorrect (or at least the projected drought is not so severe) under conditions of changing CO_2 concentrations (Greve et al., 2019, ERL; Yang et al., 2018, NCC; Roderick et al., 2015, WRR).The authors should at least discuss the potential impacts of the elevated CO_2 on their drought risk assessment in Section 4.

Reply: Thanks for this suggestion. Sorry we did not consider the impacts of increasing CO_2 concentrations on PET (and thus SPEI) in our study. This will be discussed as follows:

When calculating potential evapotranspiration based on the reference crop Penman-Monteith model, surface resistance (r_s) is fixed to 70 s/m. However, according to recent studies (e.g., Roderick et al., 2015; Yang et al., 2018), an elevated [CO_2] environment can drive stomatal closure, increasing stomatal resistance and further increasing r_s. Subsequently, this increasing r_s causes the decline in the potential evapotranspiration, especially across vegetated lands where the photo-synthetic rate is high. From this perspective, the neglect of increasing r_s may overestimate future drying condition and corresponding drought risk changes to some extent. However, on the other hand, the increase in total leaf area with [CO_2] and growing-season length can cause countervailing decreases in r_s (Greve et al., 2019). Overall, accurate and robust quantification of r_s scaling with [CO_2] still needs additionally explicit work and substantial observed data. Though the impact of r_s on the drought assessments deserves further studies, it is beyond the scope of this study. Therefore, the traditional method is used in this study to calculate PET.

This point has been discussed in the revised manuscript (Page 19, Lines 18-29).

Greve, P., Roderick, M., Ukkola, A. M., & Wada, Y. The Aridity Index under global warming. Environmental Research Letters, 2019.

Roderick, M. L., Greve, P., & Farquhar, G. D. On the assessment of aridity with changes in atmospheric CO_2. Water Resources Research, 51(7), 5450-5463, 2015.

Yang, Y., Roderick, M. L., Zhang, S., McVicar, T. R., & Donohue, R. J. Hydrologic implications of vegetation response to elevated CO_2 in climate projections. Nature Climate Change, 9(1), 44, 2019.

3. Given the relative coarseness of the CMIP5 models, I think interpolation of the results (especially bilinearly interpolated P and PET to a common resolution before calculating SPEI with them) to 1 degree spatial resolution is not appropriate. A 2 degree

common grid would be better, and would avoid effectively making up data at the much finer resolution. The authors should at least discuss the impact of interpolation on their results in the main-text.

Reply: We agree with the reviewer it may be more appropriate to re-grid the GCM outputs to 2° common grid. However, the spatial resolution of population and GDP used in this study is 0.5°×0.5°, which have to be upscaled to the same resolution of GCM outputs. But the 2° grid may be larger than the largest city in the world, thus, it is inappropriate to reflect the regional population and GDP exposures. Besides, some national territory areas are small, a finer resolution (e.g., 1°×1°) may be more appropriate to obtain reliable population and GDP exposure results at the national scale. The same spatial resolution has been used in other studies (e.g., Schneider et al., 2016; Li et al., 2018; Yang et al., 2019).

Nevertheless, in order to validate the rationality of interpolation to 1° spatial resolution, we also re-gridded the data to 2° grid and further re-conducted our studies (Figs. R5-6). Overall, there are only slight differences between the results of 1° and 2° resolution, confirming the robustness of our results.

These clarifications have been presented in the revised manuscript (Page 24, Lines 26-29; Page 25, Lines 1-9). Corresponding figures have been added in the supplementary (Figs. S15-16)

Yang, Y., Roderick, M. L., Zhang, S., McVicar, T. R., & Donohue, R. J. Hydrologic implications of vegetation response to elevated CO_2 in climate projections. Nature Climate Change, 9(1), 44, 2019.
Li, W., Jiang, Z., Zhang, X., Li, L., & Sun, Y. Additional risk in extreme precipitation in China from 1.5 C to 2.0 C global warming levels. Science Bulletin, 63(4), 228-234, 2018.
Schneider, D. P., & Reusch, D. B. Antarctic and Southern Ocean surface temperatures in CMIP5 models in the context of the surface energy budget. Journal of Climate, 29(5), 1689-1716, 2016.

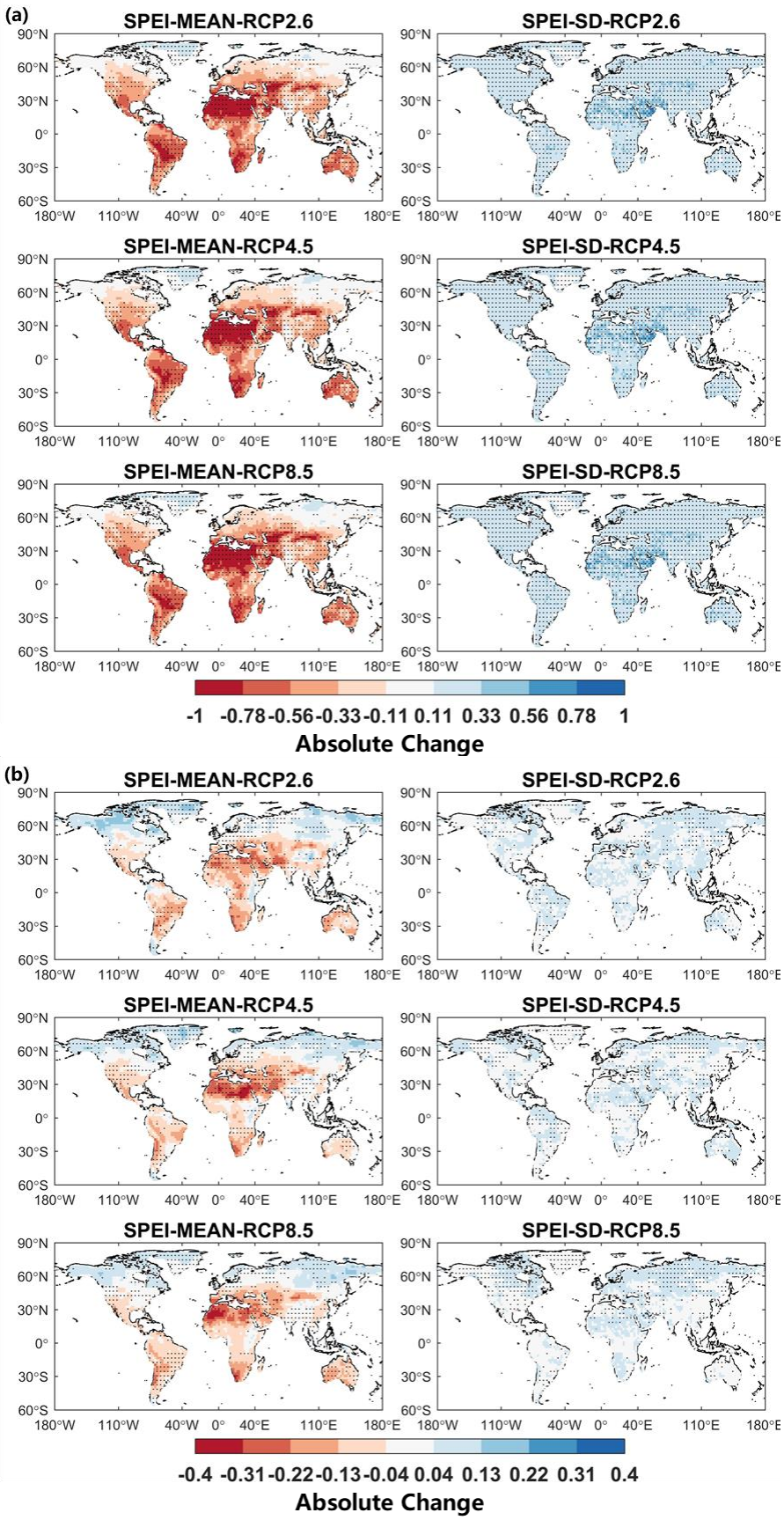

Figure R5 Projected changes in the mean and standard deviation of SPEI under the 1.5°C (a) and between the 1.5°C and 2.0°C (b) warming target at 2° spatial resolution

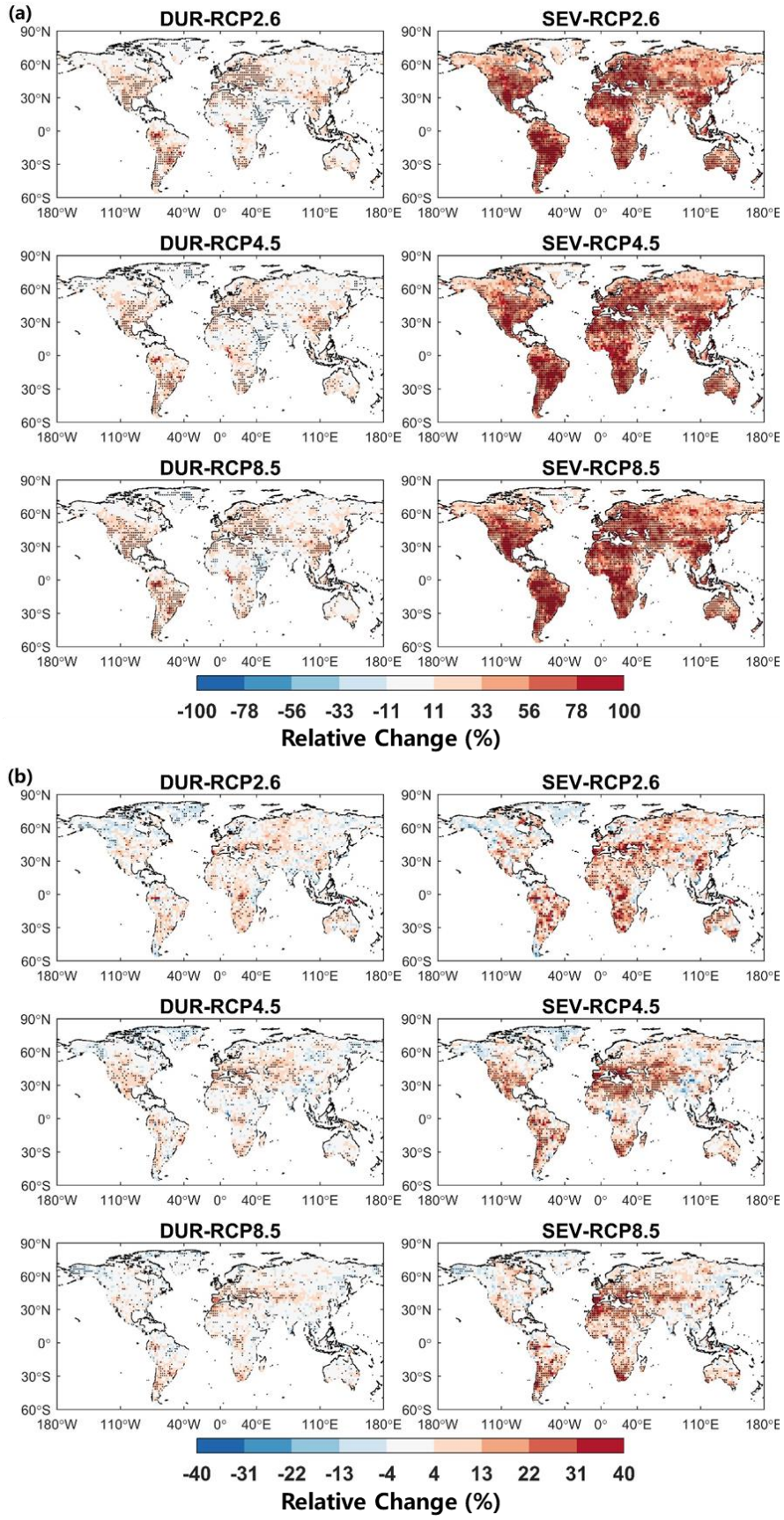

Figure R6 Projected changes in drought duration and severity under the 1.5°C (a) and between the 1.5°C and 2.0°C (b) warming target at 2° spatial resolution

Some specific parts need further clarification.

1. During the investigation regarding the exposures of population and GDP to droughts under three RCP scenarios at two warming levels, for example, under the RCP8.5 scenario (SSP5), the specific time when future warming reaches 1.5°C or 2°C under RCP 8.5 can be different (from Fig 1), population and GDP can also possibly differ in two climates. From Line 17-Line 25 (Page 11), did the author suggest that the dynamic of population and GDP under RCP 8.5 at two warming climates was also considered using the multi-year average? If so, in section 3.4 about population and GDP exposure from increasing drought risks, it was concluded that a large percentage of population and GDP will be exposed to increasing drought risk. The drought risk has been increasing with warming climate, let's say if population and GDP have been increasing with time, then which one contributes to the increasing exposures, the increasing population or the increasing drought risks, I think this is a key question that authors should clarify when assessing the socioeconomic exposure.

Reply: Thanks for this comment and sorry for the confusion of methodology of exposure analysis. We think the use of population and GDP corresponding to warming level periods instead of a single year (i.e. 2005 or 2100) which have been used by some earlier studies (e.g., Peters, 2016; Park et al., 2018; Liu et al. 2018a) may be more appropriate. The dynamic characteristics are considered as differences in population (and GDP) between the fixed 30-year 1.5°C and 2.0°C warming periods, and can be reflected by the multi-year average during warming climates to some extent (Table R1). In this way, variations in population (and GDP) and variations in drought risks can both lead to drought exposures changes. To further analyze their respective contributions, we rephrase the details as follows:

At the 1.5℃ warming climate, there are around 88% of global landmasses being exposed to increasing drought risks, which correspond to 1386.9 million population (and 33311.1 billion USD) according to the average of the three RCPs from a global perspective. At the 2.0℃ warming level, though there are still 88% of the global land areas being exposed to increasing drought risks, the affected population (and GDP) will soar to 1538.2 million (and 72852.2 billion USD). In this light, the increase in population (and GDP) contributes to the increasing exposures. Therefore, it is more appropriate to incorporate the dynamic population (and GDP) into exposure calculating processes.

When further investigating the affected population (and GDP) between the two warming climates, the role of drought risk changes should also pay attention. Specifically, though the percentage of landmasses with increasing drought risks stay unchanged for both the 1.5℃ and 2.0℃ warming climates (both approximately 88%),

the magnitudes of risk changes are different. For instance, drought risks will double across around 58% of the global landmasses at the 1.5℃ warming level, while the same drought risks will occur over 67% of the global landmasses at the 2.0℃ warming level. Those differences in the magnitudes of drought risk changes can definitely bring about divergent impacts to local population and economy.

Related information have been clarified in the revised manuscript (Page 21, Lines 26-29; Page 22, Lines 1-24).

Liu, W., Sun, F., Lim, W. H., Zhang, J., Wang, H., Shiogama, H., and Zhang, Y.: Global drought and severe drought-affected populations in 1.5 and 2 °C warmer worlds. Earth Syst. Dynam., 9:267-283, 2018a.

Park, C. E., Jeong, S. J., Joshi, M., Osborn, T. J., Ho, C. H., Piao, S., and Kim, B. M.: Keeping global warming within 1.5° C constrains emergence of aridification. Nat. Clim. Change, 8(1), 70, 2018.

Peters, G. P.: The best available science to inform 1.5 C policy choices. Nat. Clim. Change, 6(7), 646. https://doi.org/10.1038/nclimate3000, 2016.

Table R1 Global population and GDP at the 1.5℃ and 2.0℃ warming climates

	SSP126	**SSP425**	**SSP585**
1.5°C-population (million)	1516.9	1553.5	1510.8
2.0°C-population (million)	1666.7	1731.2	1603.1
1.5°C-GDP (billion USD)	35875.0	34244.0	35668.5
2.0°C-GDP (billion USD)	116991.1	56271.6	58916.2

2. Page 11, Line 13-16, how is the ratio of the recalculated recurrence frequency calculated and why a less than 1.0 ratio suggests worrisome drought condition. Need further clarification.

Reply: Sorry for the confusion. The ratio of the re-calculated recurrence frequency is based on the joint probability distribution functions. Taking the 50-year drought events as an example, we first determine the magnitudes (duration and severity) of the 50-year drought events in the historical period. Then we input the determined magnitudes of the 50-year drought events into the future joint distribution functions, recalculate the joint recurrence frequencies and convert them into new return period at the 1.5℃ and 2.0℃ warming climates. The ratio is then calculated by dividing the new return period in the 2.0℃ warming future by the new return period in the 1.5℃ warming. A ratio less than 1.0 suggests that the new return period in 2.0℃ warming climates further reduces compared to that in 1.5℃ warming level, which means that reference drought events are more common under the 0.5℃ warming impacts.

In detail, if the recurrence frequency of the 50-year event increases at the 1.5℃ warming climate, the joint return period will decrease (e.g., become 30-year event); if

the recurrence frequency of the 50-year event increases at even larger magnitudes at the 2.0℃ warming climate, the joint return period will further decrease (e.g., become 20-year event). The ratio is then calculated by dividing the re-calculated joint return period in the 2.0℃ warming level by that in the 1.5℃ warming level (i.e., 20/30). Since drought events will become more frequent with additional 0.5℃ warming, it implies worrisome conditions.

The information above has been clarified in Section 2.5 of the revised manuscript (Page 11, Lines 19-27).

3. Page 12 section 3.1 projected changes in dryness, the author used SPEI and the run theory to define drought event, and the title of the manuscript is about the global drought, why would authors use SPEI to explain the dryness instead of using the defined event to study the changes in global drought for consistency.

Reply: Thanks for this comment.

It should be noted that drought variations are different from the dryness condition under climate warming. Specifically, drought events are defined as abnormally dry conditions but cannot be used directly to explain the dryness. In other words, the projected dryness can lead to deteriorated drought conditions characterized by more frequent, longer, and more severe events, but not the other way around. Therefore, before performing drought evaluation under the rising temperature, there is a need to assess the projected climate dryness by using the drought index (i.e., SPEI). Consequently, we designed the projected changes in dryness in section 3.1 using SPEI and analyzed subsequent drought events changes in section 3.2. This framework is also consistent with previous studies (Ayantobo et al., 2017; Lehner et al., 2017). Following this procedure, the projected climatic water budget as well as the subsequent drought changes can be considered as a consequence of global warming.

Ayantobo, O.O., Li, Y., Song, S., Yao, N.: Spatial comparability of drought characteristics and related return periods in mainland China over 1961-2013. J. Hydrol., 550, 549-567, 2017.

Lehner, F., Coats, S., Stocker, T. F., Pendergrass, A. G., Sanderson, B. M., Raible, C. C., and Smerdon, J. E.: Projected drought risk in 1.5°C and 2°C warmer climates. Geophys. Res. Lett., 44: 7419-7428, 2017.

4. Page 15 Line 28-29, whether the fraction of drought-affected population (or GDP) divided by total population (or GDP) can be a fairer and more impartial assessment is really hard to say given the fact that this method seems to cover up some most drought-affected countries, like the United States and China.

Reply: Sorry for the confusion of the presentation. Instead of using the absolute value of population (and GDP) to assess the nation-wide drought exposures, we apply the nation-wide population (and GDP) fraction. That is, for a country (e.g., the United States), the fraction of drought-affected population (and GDP) divided by the total population (and GDP) of this country is employed as the indicator. Therefore, the most drought-affected countries are presented by high fractions. Moreover, the utilization of the fraction rather than the absolute value of nation-wide population (and GDP) can avoid covering up badly drought-affected countries where the national population (or GDP) are small (or low) regarding the world level.

This point has been rephrased in the revised manuscript in Page 16, Lines 1-6.

5. Generally, in the discussion of either the magnitude of drought or the socioeconomic exposures of droughts, the differences between two warming targets are highlighted, however, the differences among three RCP scenarios are barely discussed in the manuscript. It makes me doubt the reason and necessity of using three RCP scenarios since they present almost similar variations under two warming targets. This issue might be even obvious in Fig 9 and 10, for example, in Fig 9, under RCP 4.5, population and GDP suggest 100% exposure to drought in Australia, which drops to 90% under RCP 8.5. Possible reasons and texts are needed here.

Reply: Thanks for this suggestion. We give a rough discussion regarding the RCP uncertainty in Section 4 (Page 21, Lines 1-10). Though the three RCP scenarios present to some extent similar variations in terms of projected dryness patterns, there are still discernable differences in the projected drought risks and drought-affected exposures, especially when the warming increasing from the 1.5℃ to the 2.0℃ warming level (Fig. 8). Moreover, these differences will become more evident at the national scale (e.g., Figs S3-4). This will be explained as follows:

It is well-known that the warming trajectories are dependent on RCP scenarios. In other words, different RCP scenarios correspond to various temperature levels for the fixed time period. However, this study fixed the warming level. It can be expected that the differences among RCP scenarios are largely reduced. Nevertheless, the complex circulation system can still result in some differences in hydro-meteorological variables (e.g., precipitation, wind speed and relative humidity) among RCP scenarios, even at the same warming level, because they are not linearly related to the warming temperature. Since drought conditions are evaluated by using multiple hydro-meteorological variables, those differences at the same warming level can lead to variations in drought evolutions. Comparing to the middle and low emission pathway scenarios (RCP2.6 and RCP4.5), the high emission pathway scenario (RCP8.5) usually reaches the warming level at earlier time periods during which the greenhouse gas

concentrations are relatively low. In this light, the projected drought conditions and drought-affected population (and GDP) can even be slightly less severe under RCP8.5, in contrast to situations under RCP 4.5 or RCP2.6. Therefore, it is not a surprise that under RCP 4.5, population (and GDP) suggest 100% exposure to drought in Australia, while it is smaller (99.8%) under RCP 8.5.

These points have been discussed in the revised manuscript (Page 23, Lines 14-29)

6. Not sure whether section 3.5 is necessary since similar conclusions have been achieved in Fig 7 and 8, and these typical countries can just be used for further explanations in section 3.3. Besides, additional explanations for Fig 7g and Fig 8g are very necessary.

Reply: Thanks for the comment. Section 3.3 presented the global drought risk changes at grid scales; while we find for assessment at the national scale, spatially aggregating mean changes are more helpful than per-grid cell changes to indicate the risk of a particular land fraction being impacted by climate change (Fischer et al., 2013). Therefore, we investigated more thoroughly the drought-affected land fractions (Figs. 11-12) by using a binning method (Page 16, Lines 26-29) to present spatially-aggregated mean changes for eight drought-prone countries in Section 3.5. Besides, section 3.5 calculated population (and GDP) exposing to increasing drought risks at different levels (e.g., <5, 5-10, 10-20, etc.) (Figs. S3-4), which can provide more systematic exposure information than those in section 3.4 which only counts population (and GDP) exposing to increasing drought risks as a whole.

In addition, with regards to Figs 7g-8g, they actually present the world land fraction subject to drought risk changes of different magnitudes under three RCPs. Specifically, for an individual climate model output, we calculate the land fraction using the ratio of grid counts located at certain extent (e.g., <5) divided by the world land grid counts (excluding Antarctic). Each box in Figs 7g-8g is stemmed from the 13 climate models results and the circle in each box represents the multi-model ensemble median results. According to Fig. 7g, around 88% of global landmasses (presented by smaller than 50-year return period) will be subject to more frequent reference droughts. In terms of Fig. 8g, more frequent droughts (indicated by less than 1 ratio) will occur over 71% of continental areas in 2.0℃ warming level compared to 1.5℃ warming. This point will be added in Section 3.3 of the revised manuscript.

This issue has been rephrased in the revised manuscript (Page 17, Lines 20-11) and the figure captions has been added in Figs. 7g-8g.

Minor suggestions.

1. Citation of Fig. 3 somewhere between lines 21 and 22 in Page 12.

Reply: Thanks. This has been added in the revised manuscript (Page 12, Line2).

2. Writing in the manuscript should be more concise in the data and method section, e.g. Page 6 line 7, use surface maximum, mean, minimum air temperature to avoid repeat.

Reply: Thanks and this has been revised in the manuscript.

3. Table 2, extreme drought instead of extremely drought

Reply: Thanks. This has been revised.

Replies to Referee #2

Projected increases in magnitude and socioeconomic exposure of global droughts in 1.5 °C and 2 °C warmer climates

Lei Gu, Jie Chen, Jiabo Yin, Sylvia C. Sullivan, Hui-Min Wang, Shenglian Guo, Liping Zhang, and Jong-Suk Kim

We thank the anonymous reviewer for the constructive comments and suggestions. We have provided detailed responses to each comment below and will revise the manuscript accordingly. For clarity, comments are given in *italics*, and our responses are given in plain text.

Authors' responses

Legend

Reviewer's comments

Authors' responses

General Comments

In summary, motivated by the 2015 Paris Agreement proposal, this manuscript calculated global 3-month Standardized Precipitation Evapotranspiration Index (SPEI-3) based on 13 CMIP5 GCM simulations under three RCP scenarios (RCP2.6/4.5/8.5) during 1976-2100, quantified changes in global drought duration, severity and occurrence under a bivariate framework, and analyzed the drought exposures of populations and regional GDP under 3 shared socioeconomic pathways (SSPs) in future 1.5 and 2-degree warming worlds. Generally, this well written manuscript is able to portray drought evolution with different warming trajectories and provides information for climate adaptation strategies. Here I list several questions below and suggest acceptance of the manuscript after minor revision.

We appreciate that the reviewer is favor of our manuscript. Please find our specific responses below.

Minor Comments

(1) P7, L19-20. How do you determine the year in which a specific warming target is achieved? I suppose you select the median year of the 30-year period with surface

temperature closest to the warming target for each RCP (not for each RCP-GCM combination), so that the reaching year is the same for all 13 GCMs under a prescribed RCP scenario. The authors should clarify this.

Reply: Sorry for that we did not clearly clarify this point. Yes, the period is determined based on multi-model ensemble mean of temperature. Thus, the reaching year is the same for all 13 GCMs under a specific RCP scenario. However, instead of using median year of the 30-year period, we used the 30-year running-mean. In other words, we selected the 30-year period with mean temperature closest to the warming target for each RCP.

This has been clarified in the revised manuscript (in Section 2.2, Page 7, Lines 19-22).

(2) Figure 1a. I've noticed that the determined years under both scenarios (RCP2.6 and RCP8.5) are the first year (2020) of the whole period. Is it possible that for some GCM future projections, 1.5-degree warming (or even higher) has already been reached even at the beginning of the simulation period? If so, maybe it could affect the results in this manuscript.

Reply: Thanks for this comment. We acknowledge that a few individual projections among the multi-model ensemble slight exceed the 1.5-degree warming at the beginning of the simulation period (i.e. BNU-ESM, CanESM2, GFDL-CM3 and MIROC-ESM-CHEM; Table R1). We will discuss this comment as follows:

To fully consider the robustness of the results, we use the warming level of multi-model ensemble mean to serve as the warming trajectory. Firstly, comparing to the method of determining warming level by individual model output, the use of multi-model ensemble mean method involves more future projections/GCMs and thus guarantees the reliability of the conclusions (Chen et al., 2011; Mehran et al., 2014). This multi-model ensemble mean method is also consistent with some previous studies (Liu et al., 2018a, 2019; Su et al., 2018). Secondly, the application of the multi-model ensemble mean method keeps the consistency of the sample size under each RCP and for each warming level. This can exclude the differences originated from the sample size when assessing different warming level impacts or evaluating RCP uncertainty. It is true that different warming level calculating methods can result in divergent model ensembles and may thus affect the results. For example, some studies (Sanderson et al., 2017; Lehner et al., 2017) used single model to conduct climate warming impact assessments, while some studies (James et al., 2017; Thober et al., 2018) employed pooled future projections (i.e. 1.5/2.0°C) to perform analyses without considering RCP discrepancies. Future studies may explore the impacts of different warming level calculation methods, but it is beyond the scope of the current study.

This has been added in the Discussion Section Page 24, Lines 8-25.

Table R1 Models with global warming higher than 1.5°C in the 2006 year (°C)

MODEL	RCP2.6	RCP4.5	RCP8.5
BNU-ESM	1.503	1.583	1.540
CanESM2	1.594	1.479	1.692
GFDL-CM3	1.720	1.734	1.741
MIROC-ESM-CHEM	1.646	1.500	1.643

Chen, J., Brissette, F. P., Poulin, A., and Leconte, R.: Overall un- certainty study of the hydrological impacts of climate change for a Canadian watershed, Water Resour. Res., 47, W12509, https://doi.org/10.1029/2011wr010602, 2011.

James, R., Washington, R., Schleussner, C. F., Rogelj, J., & Conway, D. (2017). Characterizing half‐a‐degree difference: a review of methods for identifying regional climate responses to global warming targets. Wiley Interdisciplinary Reviews: Climate Change, 8(2), e457.

Lehner, F., Coats, S., Stocker, T. F., Pendergrass, A. G., Sanderson, B. M., Raible, C. C., and Smerdon, J. E.: Projected drought risk in 1.5°C and 2°C warmer climates. Geophys. Res. Lett., 44: 7419-7428, 2017.

Liu, W., Sun, F., Lim, W. H., Zhang, J., Wang, H., Shiogama, H., and Zhang, Y.: Global drought and severe drought-affected populations in 1.5 and 2 °C warmer worlds. Earth Syst. Dynam., 9:267-283, 2018a.

Liu, W., & Sun, F. Increased adversely-affected population from water shortage below normal conditions in China with anthropogenic warming. Science Bulletin, 64(9), 567-569, 2019.

Mehran, A., AghaKouchak, A., and Phillips, T. J.: Evaluation of CMIP5 continental precipitation simulations relative to satellite- based gauge-adjusted observations, J. Geophys. Res.- Atmos., 119, 1695–1707, https://doi.org/10.1002/2013jd021152, 2014.

Sanderson, B. M., Xu, Y., Tebaldi, C., et al.: Community climate simulations to assess avoided impacts in 1.5 and 2 °C futures. Earth Syst. Dynam., 8, 827-847, https://doi.org/10.5194/esd-8-827-2017, 2017.

Su, B., Huang, J., Fischer, T., Wang, Y., Kundzewicz, Z. W., Zhai, J., and Tao, H.: Drought losses in China might double between the 1.5° C and 2.0° C warming. P. Natl. Acad. Sci. USA., 115(42), 10600-10605, 2018.

Thober, S., Kumar, R., Wanders, N., Marx, A., Pan, M., Rakovec, O., ... & Zink, M. (2018). Multi-model ensemble projections of European river floods and high flows at 1.5, 2, and 3 degrees global warming. Environmental Research Letters, 13(1), 014003.

(3) Figure 9, 10, S2 and Discussion Section. There are several countries (e.g. the United States) will experience a decrease in POP and GDP fraction exposing to more frequent severe droughts under the 2-degree warming level compared to 1.5-degree. I will be appreciated if the author could provide possible reasons considering the increasing drought risks in these countries.

Reply: Thanks for this suggestion. Actually, countries that experience a decrease in POP and GDP exposure fraction under the 2°C warming can be attributed to the decreasing land fraction exposing to more frequent droughts. Here, we listed some example countries in Table R2 to analyze the reasons. We will add more analysis and revised clarifications in the revised manuscript (Section 3.4) as follows:

It should be noted that when climate warming climbing from 1.5°C to 2.0°C, there are some spatial heterogeneity with regards to drought exposures variations. Specifically, drought exposures for some countries (i.e., Canada) can be slightly decreased in 2°C warming level compared to 1.5°C warming level. This decrease in POP and GDP exposure fraction can be attributed to the decreasing land fraction exposing to more frequent droughts. For example, the land fraction suffering more frequent severe droughts in Canada will decrease (-12.77%) in 2.0°C warming level comparing to 1.5°C warming under RCP2.6 scenario. In other words, the additional 0.5°C warming will not lead to drought risk deterioration globally, partly due to the increasing column precipitable water with warming environment (Dong et al., 2019; Yin et al., 2019), although it holds for the majority of global land masses. Anyway, the spatial heterogeneity should be paid attention especially when assessing the climate change impacts on extreme events at regional or local scales (Liu et al., 2018b).

This has been added in the revised manuscript (Page 17, 5-18). The table has been added in the supplementary (Table S2).

Table R2 Several countries suffering decreasing POP and GDP exposure

	Land fraction exposing to more frequent droughts								
	1.5°C			**2°C**			**2-1.5°C**		
Country	**RCP2.6**	**RCP4.5**	**RCP8.5**	**RCP2.6**	**RCP4.5**	**RCP8.5**	**RCP2.6**	**RCP4.5**	**RCP8.5**
Canada	68.35%	68.82%	71.56%	55.58%	63.36%	66.92%	-12.77%	-5.46%	-4.63%
United States	86.17%	78.93%	86.89%	85.44%	80.02%	79.84%	-0.72%	1.08%	-7.05%
Colombia	85.71%	84.62%	79.12%	75.82%	93.41%	85.71%	-9.89%	8.79%	6.59%
Japan	62.16%	56.76%	62.16%	59.46%	62.16%	62.16%	-2.70%	5.41%	0.00%
	Population (million)								
	1.5°C			**2°C**			**2-1.5°C**		
Country	**SSP1**	**SSP2**	**SSP5**	**SSP1**	**SSP2**	**SSP5**	**SSP1**	**SSP2**	**SSP5**
Canada	7.97	7.91	8.27	10.50	8.95	9.57	2.53	1.04	1.30
United States	59.13	58.82	60.75	73.56	64.86	68.20	14.43	6.05	7.45
Colombia	9.41	9.67	9.33	10.20	10.84	9.88	0.79	1.17	0.56
Japan	17.82	17.63	18.12	15.48	16.53	17.95	-2.34	-1.11	-0.17
	GDP (billion USD, 2010price PPP)								
	1.5°C			**2°C**			**2-1.5°C**		
Country	**SSP1**	**SSP2**	**SSP5**	**SSP1**	**SSP2**	**SSP5**	**SSP1**	**SSP2**	**SSP5**
Canada	373.60	373.74	398.99	719.26	499.22	563.41	345.67	125.48	164.41
United States	3639.14	3517.35	3759.94	6699.26	4554.66	5118.33	3060.12	1037.32	1358.38

Colombia	192.32	184.47	191.51	617.84	296.93	311.37	425.52	112.46	119.86
Japan	575.07	553.76	590.57	873.40	620.73	730.21	298.33	66.97	139.63
Population Exposure Fraction									
	1.5°C			**2°C**			**2-1.5°C**		
Country	**SSP126**	**SSP245**	**SSP585**	**SSP126**	**SSP245**	**SSP585**	**SSP126**	**SSP245**	**SSP585**
Canada	99.25%	98.88%	98.77%	99.14%	98.32%	98.70%	-0.11%	-0.56%	-0.07%
United States	99.84%	99.60%	99.85%	99.82%	99.85%	99.84%	-0.02%	0.26%	-0.01%
Colombia	84.83%	77.64%	46.20%	57.22%	98.90%	80.06%	-27.61%	21.26%	33.87%
Japan	99.72%	97.95%	99.78%	72.89%	98.65%	99.78%	-26.82%	0.70%	0.00%
GDP Exposure Fraction									
	1.5°C			**2°C**			**2-1.5°C**		
Country	**SSP126**	**SSP245**	**SSP585**	**SSP126**	**SSP245**	**SSP585**	**SSP126**	**SSP245**	**SSP585**
Canada	99.26%	98.89%	98.79%	99.15%	98.34%	98.72%	-0.11%	-0.55%	-0.07%
United States	99.84%	99.59%	99.85%	99.82%	99.85%	99.84%	-0.02%	0.26%	-0.01%
Colombia	84.85%	77.67%	46.27%	57.27%	98.90%	80.09%	-27.58%	21.23%	33.82%
Japan	99.72%	97.95%	99.78%	72.89%	98.65%	99.78%	-26.82%	0.70%	0.00%

Dong, W., Lin, Y., Wright, J. S., Xie, Y., Yin, X., & Guo, J. Precipitable water and CAPE dependence of rainfall intensities in China. Climate Dynamics, 52(5-6), 3357-3368, 2019.
Liu, W., Lim, W. H., Sun, F., Mitchell, D., Wang, H., Chen, D., ... & Fischer, E. Global freshwater availability below normal conditions and population impact under 1.5 and 2 C stabilization scenarios. Geophysical Research Letters, 45(18), 9803-9813, 2018b.
Yin, J., Gentine, P., Guo, S., Zhou, S., Sullivan, S. C., Zhang, Y., ... & Liu, P. Reply to 'Increases in temperature do not translate to increased flooding'. Nature communications, 10(1), 1-5, 2019.

(4) P10, L26. Eq. (5) should be Eq. (11)?

Reply: Sorry for the mistake. Eq. (5) will be corrected as Eq. (11) in the revised manuscript.

(5) As the authors mentioned in Section 2.1 that RCP2.6 is associated with SSP1, I suggest the author use SSP126 instead of RCP2.6 when talking about future drought risks. Same with SSP245 and SSP585.

Reply: Thanks for this suggestion. This has been addressed in revise the statement in the manuscript and corresponding figures (Figs. 7-12; 14-15) has also been revised.

(6) Relative to huge gaps in drought characteristics for two warming targets, results under three RCP scenarios seems to have few differences (e.g. Figure 6). Maybe the authors could explain the reason in Discussion Section, or explore the possible causes

in future studies.

Reply: Thanks for this insightful comment. We have added the discussion as follows in the revised manuscript (Page 23, Lines 14-29):

It is well-known that the warming trajectories are dependent on RCP scenarios. In other words, different RCP scenarios correspond to various temperature levels for the fixed time period. However, this study fixed the warming level. It can be expected that the differences among RCP scenarios are largely reduced. Nevertheless, the complex circulation system can still result in some differences in hydro-meteorological variables (e.g., precipitation, wind speed and relative humidity) among RCP scenarios, even at the same warming level, because they are not linearly related to the warming temperature. Since drought conditions are evaluated by using such hydro-meteorological variables, those differences at the same warming level can lead to variations in drought evolutions.

Furthermore, drought variations under three RCP scenarios are even to some extent significant at the regional or national scales. For example, when the warming level increasing from 1.5°C to 2.0°C, the GDP exposure for the Colombia will decrease at the SSP126 scenario while it will increase at the SSP585. Future studies may explore their potential physical mechanisms (i.e., connecting drought evolution with land-atmosphere interactions).

Projected increases in magnitude and socioeconomic exposure of global droughts in 1.5 ℃ and 2 ℃ warmer climates

Lei Gu[1], Jie Chen[1,2*], Jiabo Yin[1*], Sylvia C. Sullivan[3], Hui-Min Wang[1], Shenglian Guo[1], Liping Zhang[1,2], Jong-Suk Kim[1,2]

[1]State Key Laboratory of Water Resources and Hydropower Engineering Science, Wuhan University, Wuhan 430072, P. R. China

[2]Hubei Provincial Key Lab of Water System Science for Sponge City Construction, Wuhan University, Wuhan, China

[3]Department of Earth and Environmental Engineering, Columbia University, New York, NY 10027, USA

* *Correspondence to*: Jie Chen (jiechen@whu.edu.cn); Jiabo Yin (jboyn@whu.edu.cn)

Abstract: The Paris Agreement sets a long-term temperature goal to hold global warming to well below 2.0°C and strives to limit to 1.5°C above preindustrial levels. Droughts with either intense severity or a long persistence could both lead to substantial impacts such as infrastructure failure and ecosystem vulnerability, and they are projected to occur more frequently and trigger intensified socioeconomic consequences with global warming. However, existing assessments targeting global droughts under 1.5°C and 2.0°C warming levels usually neglect the multifaceted nature of droughts and might underestimate potential risks. This study, within a bivariate framework, quantifies the change of global drought conditions and corresponding socioeconomic exposures for additional 1.5°C and 2.0°C warming trajectories. The drought characteristics are identified using the Standardized Precipitation Evapotranspiration Index (SPEI) combined with the run theory, with the climate scenarios projected by 13 Coupled Model Inter-comparison Project Phase 5 (CMIP5) global climate models (GCMs) under three representative concentration pathways (RCP2.6, 4.5 and 8.5). The copula functions and the most likely realization are incorporated to model the joint distribution of drought severity and duration, and changes in the bivariate return period with global warming are evaluated. Finally, the drought exposures of populations and

regional gross domestic product (GDP) under different shared socioeconomic pathways (SSPs) are investigated globally. The results show that within the bivariate framework, the historical 50-year droughts may double across 58% of global landmasses in a 1.5°C warmer world, while when the warming climbs up to 2.0℃, an additionally 9% of world landmasses would be exposed to such catastrophic drought deteriorations. More than 75 (73) countries' population (GDP) will be completely affected by increasing drought risks under the 1.5°C warming, while an extra 0.5℃ warming will further lead to an additional 17 countries suffering from a nearly unbearable situation. Our results demonstrate that limiting global warming to 1.5°C, compared with 2°C warming, can perceptibly mitigate the drought impacts over major regions of the world.
Keywords: Global warming; Drought; Copula function; Most likely scenario; Socioeconomic exposures

1. Introduction

Climate warming mainly due to greenhouse gas emissions has altered the global hydrological cycle and resulted in more frequent and persistent natural hazards such as droughts, which have imposed considerable economic, societal, and environmental challenges across the globe (Handmer et al., 2012; Chang et al., 2016; EM-DAT 2017). With the aspiration to mitigate these adverse consequences, the Paris Agreement proposed to cut greenhouse gas emissions for holding the increase in global temperature to well below 2.0°C and pursuing efforts, limiting the warming to 1.5°C above pre-industrial levels (UNFCCC, 2015). Regardless of the socioeconomic and technological achievability of the Paris Agreement goals, portraying the drought evolution with different warming trajectories would provide valuable information and references for mankind to enable appropriate adaptation strategies in a warmer future.

To examine the sensitivity of drought risks with different warming targets, numerous approaches have emerged. One way is to employ a set of ensemble simulations produced by a single coupled climate model (e.g., Community Earth System Model,

CESM), which is designed specifically to perform the impact assessments at a near-equilibrium scenarios of 1.5°C or 2°C additional warming (Sanderson et al., 2017; Lehner et al., 2017). This single model type cannot reflect the structural uncertainty of climate models, which is important in impact assessments, and thus raises doubts about the robustness of such drought condition assessments (Liu et al., 2018a). Emerging modeling efforts such as the "Half a degree Additional warming, Projections, Prognosis and Impacts" (HAPPI) model inter-comparison project provided a new dataset with experiments designed to explicitly target impacts of 1.5°C and 2°C above preindustrial warming (Mitchell et al., 2016). However, the HAPPI employed prescribed climatological sea surface temperatures and could not consider the internal variability of ocean-atmosphere circulation, which is crucial in physically simulating climatic variability and persistence (Seager et al., 2005; Routson et al., 2016). Current studies usually utilize CMIP5 climate models to project climate scenarios under different RCPs, identify the time period for a warming target and then examine the drought conditions associated with different levels of global warming. For instance, Su et al. (2018) used 13 CMIP5 models based on RCP 2.6 and RCP 4.5 to compare the drought conditions for two warming targets over China and reported tremendous losses will emerge even under the ambitious 1.5°C warming target.

These prevailing tides of literature almost reach a consensus that, with higher saturation threshold and more intense and frequent dry spells driven by rising temperatures, drought conditions would considerably worsen in many regions of the world (Mitchell et al., 2016; Liu et al., 2018a, b). The potentially devastating impacts of more severe drought conditions on society raise considerable concerns, motivating a number of global socioeconomic assessments of future drought change impact (e.g., Below et al., 2007; Schilling et al., 2012). For instance, Liu et al. (2018a) investigated global drought evolution and corresponding population exposures in additional 1.5°C and 2°C warming conditions using a set of CMIP5 models under RCP 4.5 and RCP 8.5. Naumann et al. (2018) assessed the development of drought conditions across the world for different warming targets in the Paris Agreement. These studies concluded that there

are considerable benefits for the environment and society of limiting warming to 1.5°C relative to 2.0°C, although 1.5°C warming still implies a substantial challenge for global sustainable development. However, most previous socioeconomic assessments (e.g., Peters, 2016; Park et al., 2018; Liu et al. 2019) have focused on a static socioeconomic scenario, probably due to data constraint. These studies cannot capture the dynamic nature of population and assets over time, that has been identified as crucial for simulating realistic societal development path (Smirnov et al., 2016). Recently, five Shared Socioeconomic Pathways (SSPs) have been proposed, providing a more reasonable dataset to characterize a set of plausible alternative futures of societal development with consideration of climate change and policy impacts over the 21st century (Leimbach et al., 2017). To date, the SSPs have not yet been incorporated into the drought impact assessments with warming at the global scale.

More importantly, among existing global drought impact assessments, especially those targeting different warming levels proposed by the Paris Agreement, drought variables such as severity and duration are usually separately investigated through probability modelling and stochastic theories (e.g., Sanderson et al., 2017; Lehner et al., 2017; Su et al., 2018). Knowing that droughts are multifaceted phenomena (Xu et al., 2015; Tsakiris et al., 2016) usually characterized by duration and severity, univariate frequency analysis is unable to describe the probability of occurrence for the drought events physically and may lead to underestimation of drought risks and societal hazards. For instance, droughts with a moderate severity but a long persistence are seldom identified as severe events in univariate analysis; nevertheless, they may pose substantial socioeconomic losses because of rapid stored water depletion and low resilience to subsequent droughts (Lehner et al., 2017). Therefore, there is an urgent necessity to incorporate the joint modeling of multiple drought features into impact assessments (Genest et al., 2007; Liu et al., 2015). The copula function that shows good feasibility of marginal distributions in modeling inter-correlated variables has been introduced in multivariate analysis for droughts (e.g., Wong et al. 2013; Zhang et al. 2015; Ayantobo et al., 2017). However, to the authors' knowledge, no previous work

links the high interdependence of drought characteristics to a global impact assessment under different warming levels.

In the multivariate framework, selection of variable combinations along the quantile curve poses a new challenge, as the choice of the joint return period (JRP) leads to infinitely many such combinations. To meet the needs of infrastructure design and adaptivity, many researchers (e.g., Chen et al. 2010; Li et al. 2016; Zscheischler et al., 2017) have assumed that the correlated variables have the same probability of occurrence under a given JRP, which is called the equivalent frequency combination (EFC) method. Despite the fact that the EFC method has low calculation complexity, the statistical and theoretical basis of the equal frequency assumption is questionable (Yin et al. 2018a). To develop a more rational design for a multivariate approach, a novel concept of "most likely design realization" to choose the point with the highest likelihood along the quantile curve has been proposed in frequency analysis (Salvadori et al. 2011; Yin et al. 2019). It would be very important to evaluate and characterize these different likelihoods of drought events in bivariate drought impact assessment under a warming climate.

In this study, under a bivariate framework, we quantify changes in global drought conditions and socioeconomic exposure with additional levels of 1.5°C and 2.0°C warming. The drought characteristics are identified using the Standardized Precipitation Evapotranspiration Index (SPEI) combined with the run theory and with climate scenarios simulated by 13 CMIP5 GCMs under three RCPs (RCP2.6, 4.5, and 8.5). The copula functions and most likely realization are incorporated to model the drought severity and duration concurrently, and changes in the bivariate return period with global warming are systematically investigated. Finally, the drought exposures of populations and regional GDP under different shared socioeconomic pathways (SSPs) are assessed globally.

2. Materials and Method

2.1 Climatic and socioeconomic scenarios

Climate projections are based on ensemble runs (r1i1p1) by 13 models from CMIP5 (Table 1), covering the period 1976-2100 under three RCPs (i.e., RCP 2.6, 4.5, and 8.5).

Ten climate variables were used in this study. Specifically, 9 out of the 10 variables were applied for the calculation of potential evapotranspiration (PET). These 9 variables include: surface maximum, mean, and minimum air temperatures~~, surface minimum air temperature, surface maximum air temperature~~, surface wind speed, relative humidity, surface downwelling ~~longwave flux, surface~~and upwelling longwave fluxes, surface downwelling ~~shortwave flux, and surface~~and upwelling shortwave fluxes. The 10th variable is the precipitation. Then the calculated PET and GCM-simulated precipitation were employed to calculate drought indices. The PET was initially calculated at the daily scale. Then both the daily scale PET and precipitation were aggregated to the monthly scales, and bilinearly interpolated to a spatial resolution of 1.0° × 1.0° on latitude and longitude for each model simulation.

带格式的：字体颜色：蓝色

To assess the exposures of populations and assets to droughts, which will eventually lead to higher drought losses in the future, instead of using a static socioeconomic scenario as many studies have (e.g., Hirabayashi et al., 2013; Smirnov et al., 2016), we employ the spatially explicit global shared socioeconomic pathways (SSPs). This dataset includes gridded population and GDP data under five SSPs, covering the period 2010-2100 at a spatial resolution of 0.5°×0.5° (Jiang et al., 2017; 2018; Su et al., 2018; Huang et al., 2019). It involves a sustainable scenario (SSP1), a pathway of continuing historical trend (SSP2), a strongly fragmented world (SSP3), a highly unequal world (SSP4), and a growth-oriented world (SSP5). Among combinations of different RCP trajectories and socioeconomic pathways, some SSP-RCP combinations are unlikely to occur, e.g., SSP3-RCP2.6 and SSP1-RCP8.5 (Jones

et al., 2016). Considering the socioeconomic challenges for mitigation along different development paths, the RCP2.6 scenario is associated with SSP1 (SSP126), which will face a lower challenge of mitigation in the future. The RCP4.5 scenario is associated with the SSP2 (SSP245), while the highest emission scenario RCP 8.5 is associated with the SSP5 (SSP585), by which a relatively higher challenge is expected under foreseeable warming conditions (Samir et al., 2017).

带格式的：字体颜色：蓝色

带格式的：字体颜色：蓝色

带格式的：字体颜色：蓝色

2.2. Definition of a baseline, 1.5℃ and 2℃ global warming

The sensitivity of annual global temperature to climate variability significantly varies in models and RCPs. Therefore, the time period with additional global warming of 1.5°C and 2°C with respect to pre-industrial conditions also varies between different climate scenarios. Here, the time periods for different global warming levels are determined using the 30-year running-mean of multi-model ensemble mean of global-mean surface air temperature, following previous studies (Vautard et al., 2014; Su et al., 2018). We first select a baseline period of 1976-2005, during which the observed global average temperature was approximately 0.46-0.66°C warmer than pre-industrial condition (IPCC, 2018). This reference period is widely adopted for climate impact assessment (e.g., Vautard et al., 2014), and we set the warming degree during baseline period as 0.51°C; hence the 1.5°C and 2.0°C warming targets are determined by additional warming of 0.99°C and 1.49°C, respectively. For each RCP, we define the 1.5°C and 2°C warmer worlds by using the multi-model ensemble mean of global temperature. In other words, the reaching year is the same for all 13 GCMs under a specific RCP scenario and is determined as the 30-year period with mean temperature closest to the warming target for each RCP. ~~during which the moving 30-year period with global warming closely approximates to the corresponding warming levels~~ (see Fig. 1).

带格式的：字体颜色：蓝色

2.3 Drought indices and event identification

2.3.1 Standardized Precipitation Evapotranspiration Index

The drought condition is quantified with the SPEI developed by Vicente et al. (2010), which has been widely adopted in characterizing drought conditions (e.g., Ayantobo et al., 2018; Wen et al., 2018). The SPEI quantifies the extent of atmospheric water surplus and deficit relative to the long-term average condition by standardizing the difference between precipitation and potential evapotranspiration (PET). The SPEI with 3-month time scale (SPEI-3) is used in this study because it captures well the shallow soil moisture available to crops and reflects seasonal water loss processes (Yu et al., 2014).

The PET is first calculated using the Penman-Monteith approach suggested by the Food and Agriculture Organization of the United Nations (FAO) (Allen et al., 1998):

$$PET = \frac{0.408\Delta\left(R_n - G\right) + \gamma \frac{900}{tmean + 273} u_2 \left(e_s - e_a\right)}{\Delta + \gamma\left(1 + 0.34u_2\right)} \quad (1)$$

where Δ is the slope of saturation vapor pressure vs. air temperature curve (kPa /°C) and is calculated by:

$$\Delta = 4098 \times \frac{0.6108 \times e^{\frac{17.27 \times tmean}{tmean + 237.3}}}{tmean + 237.3} \quad (2)$$

where *tmean* is the surface mean air temperature (°C). R_n is the net radiation (MJ/m^2/day) and is calculated by:

$$R_n = [rsds - rsus - (rlus - rlds)] * 10^6 * 3600 * 24 \quad (3)$$

where *rsds* and *rsus* (*rlds* and *rlus*) are surface downwelling and upwelling shortwave flux (surface downwelling and upwelling longwave flux), respectively (w/m^2). G is the soil heat flux (MJ/m^2/day) and is close to zero at the daily scale. γ is psychometric constant (kPa/°C) and is calculated by:

$$\gamma = 0.665 \times 10^{-3} \times P \quad (4)$$

where P is the atmospheric pressure (kPa). u_2 is the wind speed at 2m height (m/s), transferred from:

$$u_2 = 4.87 \times u_{10} / \ln(67.8 \times 10 - 5.42) \quad (5)$$

where u_{10} is the surface wind speed at the 10m height simulated by GCMs. e_s and e_a are saturation and actual vapor pressure (kPa), respectively:

$$e_s = 0.6108 \times e^{\frac{17.27 \times tmp}{tmp+237.3}} \quad (6)$$

$$e_a = \frac{rhs}{100} \times e_s \quad (7)$$

where *rhs* is the relative humidity (%), and *tmp* is temperature (i.e., daily maximum and minimum air temperature). Due to the non-linearity of eq. (6), it would be more appropriate to apply the average saturated vapor pressure derived from the daily maximum and minimum air temperature.

The widely used Log-logistic distribution is employed for fitting the 3-month deficit of precipitation and PET (P-PET) (Touma et al., 2015):

$$F(\mathrm{x}) = [1 + (\frac{\alpha}{x - \lambda})^{\beta}]^{-1} \quad (8)$$

where, $F(x)$ denotes the cumulative distribution function; α, β and λ represent shape, scale and location parameters, which are estimated by the maximum likelihood method (Ahmad et al., 1988).

The SPEI-3 can then be derived by standardizing the $F(x)$ into a standard normal function with a transforming function Φ^{-1} as follows:

$$SPEI_{-3}(x) = \Phi^{-1}(F(x)) \quad (9)$$

2.3.2 Drought event identification

After calculating the SPEI-3 for global terrestrial grid cells, we derive the drought duration, intensity, and severity using the run theory for the reference and the 1.5°C and 2°C warmer worlds. The run theory proposed by Yevjevich et al. (1967) is a useful and objective method for drought event identification, where a run represents a subset of time series, in which SPEI-3 is either beneath (i.e., negative run) or over (i.e., positive run) a fixed threshold. A run with SPEI-3 that continuously stays below -0.5 is defined

as a drought event (Mishra et al., 2010; Zargar et al., 2011), which generally includes drought characteristics of duration and severity. The persistent time period during a drought event is further defined as the drought duration, while drought severity (dimensionless) is defined as a cumulative deficit below -0.5.

2.4 Bivariate return period and most likely realization method

Previous studies usually independently examined the change either in drought duration or severity under climate warming, neglecting the multiplex nature of droughts (Naumann et al., 2018). This study jointly models drought duration (D) and severity (S) via the copula function, which is versatile for describing dependent hydrological variables due to its good flexibility of marginal distributions. The widely-used Gamma distribution was adopted for fitting drought variables in each grid over the globe, and we selected the Gumbel Copula to model the joint distribution of drought duration and severity. Within the copula-based approaches, different definitions of joint return periods (JRPs) have been proposed, such as OR, AND, Kendall, dynamic, structure-based return periods (Yin et al., 2019). Among these, the OR case (T_{or}) is usually adopted in drought occurrence assessment (Zhang et al., 2015):

$$T_{or} = \frac{E_l}{1 - F(d,s)} = \frac{E_l}{1 - C[F_D(d), F_S(s)]} \tag{10}$$

where, E_l represents the expected inter-arrival time of drought events, the joint distribution $F(d, s)$ could be described by a copula function $C[F_D(d), F_S(s)]$; $F_D(d)$ and $F_S(s)$ indicate the marginal distribution functions of D and S, respectively.

Under the bivariate framework, the choice of an appropriate T_{or} leads to infinite combinations of drought duration and severity. The drought events along the T_{or}-level curve are generally not equivalent in terms of environmental and societal consequences, and hence the likelihood of each event must be taken into consideration when selecting appropriate joint quantiles. In this paper, the most likely realization method (Salvadori et al., 2011; Yin et al., 2019) is used to choose the drought scenario with the highest likelihood along the T_{or}-level isoline. For a given T_{or}, the most likely combination point

among all possible events can be derived by the following formula (Gräler et al., 2013):

$$\left\{\begin{array}{l}(d^*, s^*) = \arg\max f(d,s) = c[F_D(\mathrm{d}), F_S(\mathrm{s})] f_D(\mathrm{d}) f_S(\mathrm{s}) \\ C(F_D(\mathrm{d}), F_S(\mathrm{s})) = 1 - E_l / T_{or}\end{array}\right\} \quad (11)$$

where, $f(d,s)$ represents the joint probability density function of drought duration and severity, $c[F_D(\mathrm{d}), F_S(\mathrm{s})] = dC(F_D(\mathrm{d}), F_S(\mathrm{s})) / d(f_D(\mathrm{d}))\,\mathrm{d}(f_S(\mathrm{s}))$ indicates the density function of copula; $f_D(\mathrm{d})$ and $f_S(s)$ are probability density functions of drought duration and severity, respectively. Due to the complexity of deriving analytical solutions in Eq. (11), the harmonic mean Newton's method (Yin et al., 2018a) is applied to estimate the most likely realizations.

带格式的：字体颜色：蓝色

2.5 Calculation of socioeconomic exposure under warmer condition

To calculate the socioeconomic exposures by droughts in different warming environments, we evaluate the change of drought occurrence frequency in a bivariate context. Firstly, we estimate the bivariate quantiles of drought duration and severity (i.e., most likely realization) under one given JRP during the historical period. As the 50-year drought events usually gained great attention by the scientific community and socio-climatic policymakers (Zhang et al. 2015; Naumann et al., 2018), we adopt this level as a reference for assessing possible drought implications. With the historical 50-year bivariate quantiles, we can recalculate the joint occurrence frequency under future additional 1.5℃ and 2.0℃ warming conditions, respectively. It can be inferred that areas with a JRP lower than 50 years are projected to suffer from more severe drought conditions. To explicitly assess the drought risk changes from 1.5℃ to 2.0℃ warming climates, we estimate the ratio of the recalculated recurrence frequency between these two warming periods~~:~~. Taking the 50-year drought events as an example, we first determine the magnitudes (duration and severity) of the 50-year drought events in the historical period. Then we input the determined magnitudes of the 50-year drought events into the future joint distribution functions, recalculate the joint recurrence frequencies and convert them into new return period at the 1.5℃ and 2.0℃ warming

带格式的：字体颜色：蓝色

带格式的：字体颜色：蓝色

带格式的：字体颜色：蓝色

climates. The ratio is then calculated by dividing the new return period in the 2.0℃ warming future by the new return period in the 1.5℃ warming. A ratio less than 1.0 suggests that the new return period in 2.0℃ warming climates further reduces compared to that in 1.5℃ warming level, which means that reference drought events are more common under the 0.5℃ warming impacts and implies worrisome conditions. ~~where those areas with a less than 1.0 ratio are projected to be exposed to worrisome drought conditions.~~

带格式的：字体颜色：蓝色

带格式的：字体颜色：蓝色

带格式的：字体颜色：蓝色

带格式的：字体颜色：蓝色

带格式的：字体颜色：蓝色

To evaluate socioeconomic implications of drought with additional warming, we record the population and GDP in those areas with more severe drought conditions and define them as exposures by increasing drought risks. As previously stated, we consider the dynamic nature of socioeconomic development pathways by employing different SSPs, and used the multi-year average populations and GDPs during 30-year periods determined by different warming levels. After estimating the socioeconomic exposures for each GCM simulation, we use the multi-model ensemble mean as an indication for each grid cell to reduce model bias. Note that we select three RCPs and corresponding SSPs under two warming targets so that the analysis is performed on six scenarios.

3. Results

3.1 Projected changes in dryness

We first examine changes in the mean and standard deviation of SPEI-3 from the historical reference period (1976-2005) to the 1.5℃ warmer worlds (Fig. 2), indicated by the multi-model ensemble mean results. We find that mean SPEI-3 decreases at the global scale (across 85% of the land areas, excluding Antarctica), except in very limited regions at high-latitude areas (e.g., Siberia in Russia) where it exhibits a slight increase. The descending changes in the mean SPEI-3 imply that, over the majority of the globe, the probability distribution function of SPEI-3 would shift towards lower values and hence more severe dryness. Particularly, dramatic decreases combined with strong model agreement (in terms of sign of change) are presented in Southern America, Australia, and Northern Africa. This may be attributed to higher evaporative demands

and more frequent and persistent dry spells associated with rising temperatures (Naumann et al., 2018). On the other hand, we also observe an increase in the standard deviation of SPEI-3 with additional 1.5°C warming, particularly in Northern Africa and Southwestern Asia. As the SPEI-3 follows the standard normal distribution, the increasing standard deviation means more variability in dryness, which hinders resilience efforts in a 1.5°C warmer world. These changes are consistent under three different RCPs, indicating the robustness of this globally drier future.

How would the dryness pattern change from 1.5°C to 2.0°C warming climates? A progressive descending change in mean values of SPEI-3 is observed across 58% of the land surface with the global mean temperature increasing between 1.5°C and 2.0°C, although several high-latitude regions (i.e., Russia, Canada) show an insignificant opposite change (Fig. 3). This may be mechanically explained by thick clouds in these regions that strengthen the reflectance of shortwave radiation and limit the increase of latent heat flux as well as evapotranspiration, thus contributing to the mitigation of atmospheric aridity (Huang et al., 2017). For the change in the standard deviation of SPEI-3, we find that increases occur over continental regions almost globally, accompanied by minor spatial variability. Overall, the climatic metric SPEI-3 shows a strong negative response to the warming climate, suggesting that dryness will intensify in a future warming world.

带格式的：字体颜色：蓝色

3.2 Projected changes in drought characteristics

Fig. 4 shows the relative change of global drought duration and severity derived from SPEI-3 in the 1.5°C warmer world relative to the historical period under three different RCPs. The drought duration is projected to slowly prolong with warming across 78% of the land surface, and 44% of land areas has an increase of higher than 10%, although the change is not significant in Russia and Sahel areas. The drought severity shows a much more pronounced rise globally, with significant increases (exceeding 50%) over 46% of global landmasses. Moreover, several regions experience compound increases (with strong model agreement) in both drought severity and duration, such as Southeast Asia, Mediterranean, Southern Africa, Southern North

America, and South America, suggesting an urgent need to increase societal and environmental resilience to a warming climate there. In the tropics and high-latitudes areas, the drought severity is projected to increase while the duration will decrease. In these regions, mitigation strategies should target short, intense bursts of drought.

When the global temperature rises from additional 1.5°C to 2.0°C warming, the world would experience more severe drought conditions, with a further increase in drought severity accounting for 75% of the land surface (differences in effects between the 1.5℃ and 2.0℃ warming levels) and a persistent lengthen in duration across 58% of the land areas (Fig. 5). Similar to the changing pattern from baseline to a 1.5°C warming climate, the drought severity shows a more rapidly increasing rate than drought duration globally under the 2.0°C warming world. Comparing the 2.0°C to the 1.5°C warming condition, the increase in drought severity is greater than 10% over 35% of the land areas, while only 8% of the land areas show such an increase (>10%) in drought duration. This drought-prone condition is more severe in several regions such as Mediterranean regions, South Africa and South America, posing large challenges for existing socio-hydrological systems there.

To explicitly investigate the changes of drought characteristics under warming conditions, we also show statistics of drought frequency, duration and severity in the historical period and future additional warmer worlds in violin plots (Fig. 6), in which the distributions comprise drought characteristics across all land pixels of the multi-model ensemble mean results. The violin plots (Hintze et al., 1998) consist of a boxplot inside and an outside violin shape which displays the probability distribution of drought characteristics. Apparently, the drought frequency based on SPEI-3 is also projected to pronouncedly lengthen under three RCPs, accompanied by large variability capturing by the kernel density estimation in Fig 6. This rapid increasing tendency also holds true for drought duration and severity, and extreme conditions are projected to occur more frequently under warming climates. For example, the 90% uncertainty range of drought duration (severity) increases from 2.2-6.5 months to 1.8-7.8 months (from 2.1-6.6 to 2.0-12) under 2.0°C warming climate relative to the historical period.

3.3 Projected changes in drought risks

As evidence is accumulating that high-impact events are typically multivariate in nature (Zhang et al. 2015; Ayantobo et al., 2017), we now consider a deeper focus on changes in drought severity and duration within a bivariate framework under different warming levels. Using the copula-based approach in Section 2.4, we show the median projected change of the historical 50-year drought conditions over multi-model ensembles under 1.5°C warming climate (Fig. 7). Generally, in regions with a substantial increase in drought duration and severity (Fig. 5), the 50-year drought events exhibit a rapid increase in occurrence with warming. More than 88% of global landmasses will be subject to more frequent historical 50-year droughts, and the frequency of such severe droughts would double over 58% of the global land surface. For most areas of South America (except for the zone around the equator), Northeastern America, Central, and West Asia, and northwest China, the historical 50-year droughts are projected to occur 2 to 10 times more frequently under the ambitious 1.5°C warming level. Regions with a lower frequency of historical 50-year drought event indicate a reduction in drought risks, which are only limited in Siberia, India Peninsula, and Alaska.

To closely assess the drought conditions with an extra 0.5°C warming, we derive the ratio of adjusted 50-year return period between 2.0°C and 1.5°C warming worlds (Fig. 8). In regions with a ratio of less than 1.0, the present drought events are projected to occur more frequently under the half a degree additional warming, which accounts for 71% of continental areas. In addition, the frequency of the historical 50-year droughts would double across 67% of the global landmasses under the 2.0°C warming level. That is, 9% increase of the world land areas compares to the 1.5°C warming level (i.e., 58%). Although over some regions such as northern Canada and Eastern Asia, the occurrence of the extreme droughts will be less frequent to some degree, strong rises in recurrence frequency with warming are projected to dominate large parts of Europe, the southern United States, Australia, South America, Northern Africa, and the Mediterranean.

3.4 Population and GDP exposure from increasing drought risks

To understand the socio-economic influences induced by increasing drought risks (here defined as more frequent historical 50-year events), we combine the drought projection with population and GDP information based on SSPs, and estimate exposures by droughts in the 1.5°C and 2.0°C warmer worlds. Here, instead of using the absolute value of population (and GDP) to assess the nation-wide drought exposures, the nation-wide population (and GDP) fraction is employed to avoid covering up badly drought-affected countries where the national population (or GDP) are small (or low) regarding the world level. Specifically, for a country (e.g., the United States), the fraction of drought-affected population (and GDP) divided by the total population (and GDP) of this country is employed as the indicator. Therefore, the most drought-affected countries are presented by high fractions. Globally, three ~~RCPs~~ SSPs suggest a consistent projection that large percentages of population and GDP will be exposed to increasing drought risks. In more than 67 (140) countries, 100% (50%) of both populations and GDPs are exposed to more severe droughts under the 1.5°C warming target (Fig. 9). The two socioeconomic factors of GDP and population are highly correlated (O'Neill et al., 2014). Economically prosperous regions are associated with higher population and immigration (Fig. S1); thus the drought-affected GDP exposures usually exhibit similar changing pattern with the population. In regions with low GDP and population density, even when total socioeconomic exposures to droughts seem small, droughts can still cause fatal and destructive losses for those countries if their drought resilience is poor. ~~To give a fairer and more impartial assessment of droughts' socioeconomic consequences, we define and assess the fraction of drought-affected population (or GDP) divided by total national population (or total GDP) based on different countries in a 1.5°C warming world. With this national assessment method~~In addition, we see some interesting results ~~(Fig. 9)~~. For example, the United States and China are no longer the most drought-affected countries, while 100% of the population and GDP~~GPD~~ in Mexico, Southern Europe, Middle, and Southern Africa, and Mediterranean regions (i.e., Turkey, Ukraine) are projected to experience more severe

带格式的：字体颜色：蓝色

带格式的：字体颜色：蓝色

drought, suggesting large policy challenges there.

To illustrate the consequences of limiting warming to 2.0°C above the preindustrial levels, we also calculate the socioeconomic exposures under three ~~RCPs,~~SSPs (Fig. 10) and the differences in percentage between the 1.5°C and 2.0°C warming levels (Fig. S2). Most regions of the globe are projected to exhibit a generally increasing fraction (relative to 1.5°C warming) in populations and GDPs (except for Central Africa and East Asia). To be specific, under the extra half-degree warming, an additional 17 countries are projected to exhibit a 100% fraction in socioeconomic exposure. More than 10 countries would experience a 30% increase in population and GDP exposure if the global warming level increased from 1.5°C to 2.0°C. These increases illustrate the benefit of holding global warming to 1.5°C instead of 2°C, particularly for the mitigation of population and GDP exposure to drought. It should be noted that when climate warming climbing from 1.5°C to 2.0°C, there are some spatial heterogeneity with regards to drought exposures variations. Specifically, drought exposures for some countries (i.e., Canada) can be slightly decreased in 2°C warming level compared to 1.5°C warming level. This decrease in population and GDP exposure fraction can be attributed to the decreasing land fraction exposing to more frequent droughts (Table S2). For example, the land fraction suffering more frequent severe droughts in Canada will decrease (-12.77%) in 2.0°C warming level comparing to 1.5°C warming under SSP126 scenario. In other words, the additional 0.5°C warming will not lead to drought risk deterioration globally, partly due to the increasing column precipitable water with warming environment (Dong et al., 2019; Yin et al., 2019b), although it holds for the majority of global land masses. Anyway, the spatial heterogeneity should be paid attention especially when assessing the climate change impacts on extreme events at regional or local scales (Liu et al., 2018b).

3.5 National assessment of socioeconomic exposure in typical countries

The ~~drought risks and socioeconomic exposures under warming climates exhibit~~ large spatial variability~~, which~~ of drought risks and socioeconomic exposures under climate warming motivates a more systematic and in-depth assessment on national

带格式的：字体颜色：蓝色

带格式的：字体颜色：蓝色

带格式的：字体颜色：蓝色

scales, particularly for the countries vulnerable to droughts. Therefore, we investigate more thoroughly the drought-affected land fractions (Figs. 11-12) and corresponding socioeconomic exposure (Figs. S3-4) in eight hotspot countries spanning different socio-climatic regions: Argentina, Australia, Canada, China, United States, South Africa, Brazil, and Mexico.

For assessment at the national scale, spatially aggregating mean changes are more helpful than per-grid cell changes to indicate the risk of a particular land fraction being impacted by climate change (Fischer et al., 2013; Lehner et al., 2017). The land fractions of each grid cell are binned and plotted against the change of drought return period (relative to historical 50-year drought) (Figs. 11-12). The bin number is fixed to 20 groups for the eight example countries. In a 1.5°C warming world (Fig. 11), these spatially aggregated changes explicitly show a significant increase in drought risks over these hotspot countries, with more than 90% of grid cells projected to suffer from more frequent droughts.

Nevertheless, we still observe a difference between the tropics and extratropical regions. The increasing drought risks are more profound in tropical regions (e.g., Mexico and Brazil) than those over the high-latitude country (e.g., Canada). For instance, in a 1.5°C warming world, more than 85% of the grid cells (associated with around 65%-97% of the national populations and GDPs) over Mexico and Brazil could be exposed to the historical 50-year drought every 20 years. This pronounced increase in drought risks over tropical countries may be attributed to an oceanic forcing that favors the formation of deep convection over the ocean and thus weakened the continental convergence associated with the monsoon (Giannini et al., 2013). This finding suggests that the tropics may confront more severe, frequent droughts and worse socioeconomic influences (Figs. S3-4) under a warming climate. When the additional warming target rises up to 2.0°C, drought conditions worsen over all these example countries (Fig. 12). The increase in drought risks is still more pronounced in the tropical countries. More than 90% of the grid cells (associated with around 90%-100% of the national population and GDP) across Brazil and Mexico will experience drought

frequency double that of the historical 50-year drought.

Overall, increasing drought risks under warming climates can cause major challenges for sustainable development and existing infrastructure systems, while ambitiously limiting warming to 1.5°C would substantially mitigate future drought risks and corresponding socioeconomic exposures.

4. Discussion

Among the warming-induced hydrological changes, one of the most definitive and detectable changes is the simultaneous increase of precipitation and evaporative demand, which are governed by the Clausius-Clapeyron relationship (Scheff et al., 2014). Observations and model simulations have reported a variety of scaling rates between precipitation and global temperature, where the daily and hourly precipitation extremes (i.e., 99^{th} / 95^{th} percentile precipitation) usually exhibit a sub C-C scaling at regional scales, accompanied by spatial and decadal variability (Yin et al. 2018b). For global average precipitation, however, most climate models project an increase of 1-3% per degree warming (Liu et al., 2013). This deviation from the C-C relation law is due to a global radiative energy constraint (Held et al., 2006) and atmospheric moisture limitation by decreasing relative humidity and increasing the potential for intense tropical and subtropical thunderstorms under warming (Muller et al., 2011; Yin et al. 2018b). Potential evapotranspiration, on the other hand, is predicted to increase by 1.5-4% per degree warming (Scheff et al., 2014; Naumann et al., 2018). Therefore, we expect climate warming to lead to a general intensification of drought conditions, as the drying of the surface is enhanced with water scarcity. This is confirmed by the decreasing SPEI-3 and significantly increasing drought severity and duration with warming globally found here (Figs. 2-8).

The reference crop Penman-Monteith model is employed to calculate potential evapotranspiration (and thus SPEI) in the current study. In this process, surface resistance (r_s) is fixed to 70 s/m. However, according to recent studies (e.g., Roderick et al., 2015; Yang et al., 2018), an elevated CO_2 environment can drive stomatal closure,

带格式的：字体颜色：蓝色
带格式的：字体：倾斜，字体颜色：蓝色
带格式的：字体：倾斜，字体颜色：蓝色，下标
带格式的：字体颜色：蓝色
带格式的：字体颜色：蓝色，下标
带格式的：字体颜色：蓝色

increasing stomatal resistance and further increasing r_s. Subsequently, this increasing r_s causes the decline in the potential evapotranspiration, especially across vegetated lands where the photo-synthetic rate is high. From this perspective, the neglect of increasing r_s may overestimate future drying condition and corresponding drought risk changes to some extent. However, on the other hand, the increase in total leaf area with CO_2 and growing-season length can cause countervailing decreases in r_s (Greve et al., 2019). Overall, accurate and robust quantification of r_s scaling with CO_2 still needs additionally explicit work and substantial observed data. Though the impact of r_s on the drought assessments deserves further studies, it is beyond the scope of this study. Therefore, the traditional fixed r_s method is used in this study to calculate potential evapotranspiration.

In the run theory, once the threshold (e.g., -0.5) is determined, drought events with different severity magnitudes are identified and constitute a sample for the selected time period. This sample contains different magnitudes in severity and different lengths in the duration, therefore, characterizes the distribution of different levels of drought (ranging from the mild, moderate to extreme conditions). On the other hand, ~~D~~different threshold values in identifying a drought event may cause disparities regarding drought risk changes and may challenge the robustness of our results. Generally, the threshold value usually ranges between -1 and 0 (Xu et al., 2015; Ayantobo et al., 2017, 2018; Yuan et al., 2017; Jiao et al., 2019). Herein, the threshold of -0.5 is employed to identify droughts varying from mild to extremely dry levels (Table 2, Chen et al., 2018), which has been widely adopted in drought-related studies (Liu et al., 2015; Xiao et al., 2017; Chen et al., 2018). The inclusion of minor drought events can enlarge the sample size in bivariate frequency analysis and thus circumvents the problem of insufficient samples. Moreover, to verify the robustness of our results, we also use the -0.8 threshold to serve as a comparison. Relevant results are shown in Figs. 13-15. Fig.13 displays comparisons of distributions comprising drought characteristics (i.e. drought frequency, drought duration and drought severity) across all land pixels between using the -0.8 and -0.5 as the threshold. Figs. 14-15 show comparisons of projected changes in joint 50-

year return periods of droughts between using the -0.8 and -0.5 as the threshold under different warming levels. As shown in the figure (Fig.13), drought characteristics tend to slightly decrease across different periods. However, future drought risk changes as indicated by the 50-year joint return period deriving from the -0.8 threshold are similar to those from the -0.5 threshold (Figs. 14-15). In addition, we also derive changes in drought risks for the 20-year or 100-year drought events to explore risk variations caused by different extents of drought (Figs. S5-6). Results shows that although the magnitudes of changes are different, they present quite similar spatial patterns. Furthermore, since the calculation of socioeconomic exposures to droughts is based on the variations of drought risks when employing the same dynamic population (and GDP) pathways, similar changes in the drought risks will lead to analogical socioeconomic exposures. As a reference, we also analyze the socioeconomic exposures in the case when -0.8 is used as the threshold (Figs. S7-8). Compared with the results of the -0.5 threshold (Figs. 9-10), the overall characteristics of the drought exposures are mostly the same. This confirms the conclusions of our study.

带格式的：字体颜色：蓝色

Although aggravated drought risks are projected globally, the changing patterns exhibit large spatial variability, with more significant increases over mid-latitudes and tropical regions than those over high-latitude landmasses. It should be noticed that regions (e.g., the Mediterranean, Southern Africa, Southern North America) with large projected changes generally display strong model agreement (in terms of sign of change), which implies high confidence in these drought prone areas. Conversely, substantial model uncertainty of drought projections is particularly clear for regions with small changing amplitudes, as indicated by weak model agreement (e.g., Southeastern Asia and Russia). For example, 100% of the population in tropical regions like Brazil and Mexico would be affected by increasing drought risks. Indeed, our finding that the tropical and mid-latitude regions, where the vast majority of global population resides, would bear the greatest drought risks should be precautious under the foreseeable warming future. Previous studies have reported that the increases in El Niño frequency (Xie et al., 2010), an extension of Hadley cell (Lu et al., 2007), and

poleward moisture transport by transient eddies (Chou et al., 2009) under warming all contribute to the drying tendency in tropics; however, our work does not quantitatively examine these underlying physical mechanisms behind the spatial variability due to paucity of data.

When investigating ~~Moreover,~~ socioeconomic exposure (i.e., population and GDP) under different warming levels ~~is investigated in this work. Generally~~, we notice that drought ~~conditions~~ risks and population (GDP) both contribute to the exposure change. However, the use of population and GDP for a single year (i.e. 2005 or 2100) which have been used by some earlier studies (e.g., Peters, 2016; Park et al., 2018; Liu et al. 2018a) have ignored the role of dynamic socio-economic impacts. This ignoration may lead to biased conclusions. In this study, the dynamic characteristics are considered as differences in population (and GDP) between the fixed 30-year 1.5°C and 2.0°C warming periods, and can be reflected by the multi-year average during warming climates to some extent (Table 3). ~~we mainly focus on the consequences derived from drought risk changes under different warming levels.~~ Accordingly, the exposure is defined as the number of people (GDP) being exposed to areas where the bivariate drought risks increase under the warming climate. At the 1.5°C warming climate, there are around 88% of global landmasses being exposed to increasing drought risks, which correspond to 1386.9 million population (and 33311.1 billion USD) according to the average of the three RCPs from a global perspective. At the 2.0°C warming level, though there are still 88% of the global land areas being exposed to increasing drought risks, the affected population (and GDP) will soar to 1538.2 million (and 72852.2 billion USD). In this light, the increase in population (and GDP) contributes to the increasing exposures. Therefore, it is more appropriate to incorporate the dynamic population (and GDP) into exposure calculating processes. However, when further investigating the affected population (and GDP) between the two warming climates, the role of drought risk changes should also pay attention. Specifically, though the percentage of landmasses with increasing drought risks stay unchanged for both the 1.5°C and 2.0°C warming climates (both approximately 88%), the magnitudes of risk

带格式的：字体颜色：蓝色

带格式的：字体颜色：蓝色

带格式的：字体颜色：蓝色

带格式的：字体颜色：蓝色

带格式的：字体颜色：蓝色

带格式的：字体颜色：蓝色

带格式的：字体颜色：蓝色

changes are different. For instance, drought risks will double across around 58% of the global landmasses at the 1.5°C warming level, while the same drought risks will occur over 67% of the global landmasses at the 2.0℃ warming level. Those differences in the magnitudes of drought risk changes can definitely bring about divergent impacts to local population and economy. Therefore, our study strengthens the benefits and necessity of controlling the global warming at 1.5℃ level. ~~The results indicate that drought risks represented by the joint return period will significantly increase under the 1.5°C warming level and thus lead to severe impacts on the population (GDP). Furthermore, an extra 0.5°C warming will result in increasing drought risks, and at the same time, with ascending population (GDP), the exposure risk will become more awful. Though not all the land areas (71% of global landmasses) show increasing drought risks when the warming increases from 1.5°C to 2.0°C, a further 9% increase in population (119% increase in GDP) will result in a greater increase in the exposure and subsequently bring about more unbearable socio-economic consequences. Extracting contributions from population (GDP) and drought risk changes to the exposure variations is beyond the scope of this study. However, to better serve for mitigation and adaptation strategies, there is a need to systematically partition their relative contributions in future studies.~~

~~Although aggravated drought risks are projected globally, the changing patterns exhibit large spatial variability, with more significant increases over mid-latitudes and tropical regions than those over high-latitude landmasses. It should be noticed that regions (e.g., the Mediterranean, Southern Africa, Southern North America) with large projected changes generally display strong model agreement (in terms of sign of change), which implies high confidence in these drought prone areas. Conversely, substantial model uncertainty of drought projections is particularly clear for regions with small changing amplitudes, as indicated by weak model agreement (e.g., Southeastern Asia and Russia). For example, 100% of the population in tropical regions like Brazil and Mexico would be affected by increasing drought risks. Indeed, our finding that the tropical and mid-latitude regions, where the vast majority of global~~

带格式的：字体颜色：蓝色

~~population resides, would bear the greatest drought risks should be precautious under the foreseeable warming future. Previous studies have reported that the increases in El Niño frequency (Xie et al., 2010), an extension of Hadley cell (Lu et al., 2007), and poleward moisture transport by transient eddies (Chou et al., 2009) under warming all contribute to the drying tendency in tropics; however, our work does not quantitatively examine these underlying physical mechanisms behind the spatial variability due to paucity of data.~~

For a complete analysis of climate change impact assessment, it is important to know the role of corresponding uncertainty especially induced by Global Climate Models (GCMs) and RCP scenarios. ~~Besides the spatial variability of drought conditions and socioeconomic exposures, the uncertainty induced by Global Climate Models (GCMs) and RCP scenarios also plays an important role in climate impact assessment.~~ Measured by the 90% range of the changing characteristics of SPEI-3 from historical to 1.5°C warming world and from 1.5°C to 2.0°C warming target, the uncertainty induced by multi-model ensembles are quantified in each grid under three RCPs (Figs. ~~S5~~S9-~~6~~10). Compared with the ensemble mean change of SPEI-3 shown in Figs. 2-3, we find that the model uncertainty is relatively large, particular for South America and Africa where the 90% range even exceeds the ensemble mean change. This finding also holds true when evaluating the drought duration and severity (Figs. ~~S7~~S11-~~8~~12), suggesting that model uncertainty cannot be ignored in climate change impact studies.

To fully consider model uncertainty on drought conditions, we also present the bivariate return period of the present 50-year drought condition for each model under RCP 4.5 in a 1.5°C warming world, and the occurrence change under an additional 0.5°C warming (Figs. ~~S9~~S13-~~10~~14). As expected, different climate models show large variations, and several models even exhibit opposite changes over certain regions. Despite this uncertainty, most models still project general increasing risks at the global scale under climate warming, particularly for middle-latitude areas and tropics. For RCP uncertainty, although we notice that the three scenarios present similar variations

带格式的：字体颜色：蓝色

带格式的：字体颜色：蓝色

带格式的：字体颜色：蓝色

带格式的：字体颜色：蓝色

to some extent, there are still discernable differences especially when the warming increasing from the 1.5℃ to the 2.0℃ warming level. Generally, the warming trajectories are dependent on RCP scenarios. In other words, different RCP scenarios correspond to various temperature levels for the fixed time period. However, this study fixed the warming level. It can be expected that the differences among RCP scenarios are largely reduced. Nevertheless, the complex circulation system can still result in some differences in hydro-meteorological variables (e.g., precipitation, wind speed and relative humidity) among RCP scenarios, even at the same warming level, because they are not linearly related to the warming temperature. Since drought conditions are evaluated by using such hydro-meteorological variables, those differences at the same warming level can lead to variations in drought evolutions. Furthermore, drought variations under three RCP scenarios are even to some extent significant at the regional or national scales. For example, when the warming level increasing from 1.5°C to 2.0°C, the GDP exposure for the Colombia will decrease at the SSP126 scenario while it will increase at the SSP585. Future studies may explore their potential physical mechanisms (i.e., connecting drought evolution with land-atmosphere interactions). For other uncertainty sources, ~~S~~several previous studies (Wang et al., 2018; Gu et al., 2019; Chen et al., 2019) have been devoted to detecting and attributing uncertainty to GCM structure, RCPs, internal climate variability, and even drought indices and so on. Here, it is challenging to consider all these uncertainties systematically; future work could focus on including the integrated uncertainty and quantifying relative contributions on drought evolution and impact assessments.

Finally, there are some extra issues need to pay attention. For instance, to fully consider the robustness of the results, we use the warming level of multi-model ensemble mean to serve as the warming trajectory. Firstly, comparing to the method of determining warming level by individual model output, the use of multi-model ensemble mean method involves more future projections/GCMs and thus guarantees the reliability of the conclusions (Chen et al., 2011; Mehran et al., 2014). This multi-model ensemble mean method is also consistent with some previous studies (Liu et al.,

带格式的：字体颜色：蓝色

带格式的：引用 字符，字体颜色：蓝色

带格式的：字体颜色：蓝色

带格式的：引用 字符，字体颜色：蓝色

2018a, 2019; Su et al., 2018). Secondly, the application of the multi-model ensemble mean method keeps the consistency of the sample size under each RCP and for each warming level. This can exclude the differences originated from the sample size when assessing different warming level impacts or evaluating RCP uncertainty. It is true that different warming level calculating methods can result in divergent model ensembles and may thus affect the results. For example, some studies (Sanderson et al., 2017; Lehner et al., 2017) used single model to conduct climate warming impact assessments, while some studies (James et al., 2017; Thober et al., 2018) employed pooled future projections (i.e. 1.5/2.0°C) to perform analyses without considering RCP discrepancies. Future studies may explore the impacts of different warming level calculation methods, but it is beyond the scope of the current study.

In addition, considering the relative coarseness of the CMIP5 models, it may be more appropriate to re-grid the GCM outputs to a common rough grid (e.g., 2°). However, the spatial resolution of population and GDP used in this study is 0.5°×0.5°, which have to be upscaled to the same resolution of GCM outputs. But a coarse grid may be larger than the largest city in the world, thus, it is inappropriate to reflect the regional population and GDP exposures. Besides, some national territory areas are small, a finer resolution (e.g., 1°×1°) may be more appropriate to obtain reliable population and GDP exposure results at the national scale. The same spatial resolution has been used in other studies (e.g., Schneider et al., 2016; Li et al., 2018; Yang et al., 2019). Nevertheless, in order to validate the rationality of interpolation to 1° spatial resolution, we also re-gridded the data to 2° grid and further re-conducted our studies (Figs. S15-16). Overall, there are only slight differences between the results of 1° and 2° resolution, confirming the robustness of our results.

带格式的：字体颜色：蓝色

带格式的：引用 字符，字体颜色：蓝色

带格式的：字体颜色：蓝色

带格式的：引用 字符，字体颜色：蓝色

带格式的：字体颜色：蓝色

带格式的：字体颜色：蓝色

5. Conclusions

Motivated by the 2015 Paris Agreement proposal, we quantify the changes in global drought bivariate magnitudes and socioeconomic consequences in the 1.5°C and

2.0°C warmer worlds, with climate projected by the multi-model ensemble under three representative concentration pathways (RCP2.6, 4.5, and 8.5). The drought characteristics are identified using the SPEI combined with the run theory, and the changes in occurrence are measured by both drought duration and severity, with the incorporation of the copula functions and most likely realization method. The main conclusions are summarized as follows (Table S1):

(1) The mean of SPEI-3 from the historical period to the 1.5℃ and 2.0℃ warmer worlds are projected to descend at a global scale, while the standard deviation exhibits large increases. As the SPEI-3 following the normal distribution, these changes suggest that the distribution of SPEI-3 would shift towards the negative side with a flatter tendency, implying a more severe drying condition in a future warming world.

(2) The drought duration is projected to slowly prolong across 78% of the land surface, while the drought severity shows a much more pronounced rise globally in the 1.5℃ warming world. Compared to 1.5°C warming condition, there will be a further increase in drought severity and a persistent lengthening in drought duration under the additional 2.0°C warming level. Several regions in middle-latitude regions and the tropics would experience substantial increases in drought magnitude, such as Southeast Asia, the Mediterranean, Southern Africa, Southern North America, and South America.

(3) More than 58% of global landmasses would be subject to twice more frequent historical 50-year droughts even under the ambitious 1.5°C mitigation target. The drought condition will further worsen under 2.0°C warming climate, with around a 9% increase of the world landmasses experiencing such severe deterioration comparing to the 1.5°C warming level.

(4) More than 75 (73) countries are projected to exhibit a 100% fraction in the population (GDP) exposed to increasing drought risks even under the ambitious 1.5℃ warming trajectories. An extra 0.5℃ warming will lead to an additional 17 countries exhibiting a 100% fraction in socioeconomic exposure. Moreover, tropical countries (i.e., Mexico and Brazil) will be subject to dramatically increased drought risks, with 85% of the land fraction would experiencing a doubled frequency of severe historical

droughts under the 1.5℃ warming target; when the warming is increasing to 2.0℃, the corresponding land fraction is projected to approach 90%.

Data availability

The climate simulation data can be accessed from the CMIP5 archive (https://esgf-node.llnl.gov/projects/esgf-llnl/). The SSP data are provided by Prof. Buda Su and Prof. Tong Jiang in National Climate Center, China Meteorological Administration.

Author contributions

JC conceived the original idea, and LG designed the methodology. JC, LPZ and JSK collected the data. LG developed the code and performed the study, with some contributions from JC and HMW. LG, JC, JBY, SCS and SLG contributed to the interpretation of results. LG and JBY wrote the paper, and JC, SCS, SLG, LPZ and JSK revised the paper.

Conflict of interest

The authors declare that they have no conflict of interest with the work presented here.

Acknowledgements

This work was partially supported by the National Key Research and Development Program of China (No. 2017YFA0603704; 2016YFC0402206), the National Natural Science Foundation of China (Grant Nos. 51779176, 51539009, 51811540407), the Overseas Expertise Introduction Project for Discipline Innovation (111 Project) funded by Ministry of Education and State Administration of Foreign Experts Affairs P.R. China (Grant No. B18037), and the Thousand Youth Talents Plan from the Organization Department of CCP Central Committee (Wuhan University, China). The authors would

like to thank the World Climate Research Program working group on Coupled Modelling, and all climate modeling institutions listed in Table 1 for making GCM outputs available. We also thank Prof. Buda Su and Prof. Tong Jiang in National Climate Center, China Meteorological Administration for sharing the SSP data.

References

Ahmad, M. I., Sinclair, C. D., and Werritty, A.: Log-logistic flood frequency analysis. J. Hydrol., 98(3-4), 205-224, 1988.

Allen, R. G., Pereira, L. S., Raes, D., and Smith, M.: Crop evapotranspiration-Guidelines for computing crop water requirements-FAO Irrigation and drainage paper 56. Fao, Rome, 300(9), D05109, 1998.

Ayantobo, O.O., Li, Y., Song, S., Yao, N.: Spatial comparability of drought characteristics and related return periods in mainland China over 1961-2013. J. Hydrol., 550, 549-567, 2017.

Ayantobo, O. O., Li, Y., Song, S., Javed, T., & Yao, N. Probabilistic modelling of drought events in China via 2-dimensional joint copula. Journal of hydrology, 559, 373-391, 2018.

Below, R., Grover-Kopec, E. and Dilley, M.: Documenting drought-related disasters: a global reassessment. J. Environ. Dev., 16, 328-344, 2007.

Chang, J., Li, Y., Wang, Y. and Yuan, M.: Copula-based drought risk assessment combined with an integrated index in the Wei River Basin, China. J. Hydrol., 540, 824-834, 2016.

Chen, J., Brissette, F. P., Poulin, A., and Leconte, R.: Overall un- certainty study of the hydrological impacts of climate change for a Canadian watershed, Water Resour. Res., 47, W12509, https://doi.org/10.1029/2011wr010602, 2011.

Chen, J., Liu, Y., Pan, T., Liu, Y., Sun, F., & Ge, Q. Population exposure to droughts in China under the 1.5° C global warming target. Earth System Dynamics, 9(3), 1097-1106, 2018.

Chen, L., Guo, S., Yan, B., Liu, P., and Fang, B.: A new seasonal design flood method based on bivariate joint distribution of flood magnitude and date of occurrence. Hydrol. Sci. J., 55(8), 1264-1280, 2010.

Chou, C., Neelin, J. D., Chen, C. A., and Tu, J. Y.: Evaluating the "rich-get-richer" mechanism in tropical precipitation change under global warming. J. Clim., 22(8), 1982-2005. https://doi.org/10.1175/2008JCLI2471.1, 2009.

Chen, J. and Brissette, F. P.: Reliability of climate model multi‐member ensembles in estimating internal precipitation and temperature variability at the multi‐decadal scale. Int. J. Climatol., 39(2), 843-856, 2019.

Dong, W., Lin, Y., Wright, J. S., Xie, Y., Yin, X., & Guo, J. Precipitable water and CAPE dependence of rainfall intensities in China. Climate Dynamics, 52(5-6), 3357-3368, 2019.

EM-DAT.: EM-DAT: The OFDA/CRED international disaster database (Univ Catholique de Louvain, Brussels). Available at https://www.emdat.be. Accessed September 15, 2018.

Fischer, E. M., Beyerle, U., and Knutti, R.: Robust spatially aggregated projections of climate extremes. Nat. Clim. Change, 3(12), 1033, 2013.

Genest, C. and Favre, A.C.: Everything you always wanted to know about copula modelling but were afraid to ask. J. Hydrol. Eng., 12 (4), 347-368, 2007.

Giannini, A., Saravanan, R., and Chang, P.: Oceanic forcing of Sahel rainfall on interannual to interdecadal time scales. Science, 302(7): 1027-1030, 2013.

Gräler, B., van den Berg, M., Vandenberghe, S., Petroselli, A., Grimaldi, S., De Baets, B., and Verhoest, N.: Multivariate return periods in hydrology: a critical and practical review focusing on synthetic design hydrograph estimation. Hydrol. Earth Syst. Sci., 17(4), 1281-1296, 2013.

Greve, P., Roderick, M., Ukkola, A. M., & Wada, Y. The Aridity Index under global warming. Environmental Research Letters, 2019.

Gu, L., Chen, J., Xu, C. Y., Kim, J. S., Chen, H., Xia, J., and Zhang, L.: The contribution of internal climate variability to climate change impacts on droughts. Sci. Total Environ., 684, 229-246, 2019.

Handmer J, et al.: Changes in impacts of climate extremes: Human systems and ecosystems. Managing the Risks of Extreme Events and Disasters to Advance Climate Change Adaptation. A Special Report of Working Groups I and II of the Intergovernmental Panel on Climate Change (IPCC), eds Field CB, et al. (Cambridge Univ Press, Cambridge, UK), 231-290, 2012.

Held, I. M. and Soden, B. J.: Robust responses of the hydrological cycle to global warming. J. Climate, 19(21), 5686-5699, 2006.

Hintze, J. L. and Nelson, R. D.: Violin plots: a box plot-density trace synergism. The American Statistician, 52(2), 181-184, 1998.

Hirabayashi, Y., Mahendran, R., Koirala, S., Konoshima, L., Yamazaki, D., Watanabe, S., and Kanae, S.: Global flood risk under climate change. Nat. Clim. Change, 3(9), 816, 2013.

Huang, J., Yu, H., Dai, A., Wei, Y., and Kang, L.: Drylands face potential threat under 2 °C global warming target. Nat. Clim. Change, 7(6), 417, 2017.

Huang, J., Qin, D., Jiang, T., Wang, Y., Feng, Z., Zhai, J., and Su, B.: Effect of Fertility Policy Changes on the Population Structure and Economy of China: From the Perspective of the Shared Socioeconomic Pathways. Earth's Future, 7(3), 250-265, 2019.

Hulme, M.: 1.5 °C and climate research after the Paris Agreement. Nat. Clim. Change, 6, 222, 2016.

Intergovernmental Panel on Climate Change (IPCC), 2018. Special Report on Global Warming of 1.5°C.

James, R., Washington, R., Schleussner, C. F., Rogelj, J., & Conway, D. (2017). Characterizing half‐a‐degree difference: a review of methods for identifying regional climate responses to global warming targets. Wiley Interdisciplinary Reviews: Climate Change, 8(2), e457.

Jiang, T., Zhao, J., Jing, C., Cao, L. G., Wang, Y. J., Sun, H. M., and Wang, R.: National and provincial population projected to 2100 under the shared socioeconomic pathways in China. Clim. Chang. Res, 13, 128-137, 2017.

Jiang, T., Zhao, J., Cao, L., Wang, Y., Su, B., Jing, C., and Gao, C.: Projection of national and provincial economy under the shared socioeconomic pathways in China. Advances in Climate Change Research, 14(1), 50-58, 2018.

Jiao, Y., & Yuan, X. More severe hydrological drought events emerge at different warming levels over the Wudinghe watershed in northern China. Hydrology and Earth System Sciences, 23(1), 621-635, 2019.

Jones, B. and O'Neill, B. C.: Spatially explicit global population scenarios consistent with the Shared Socioeconomic Pathways. Environ. Res. Lett., 11(8), 084003, 2016.

Lehner, F., Coats, S., Stocker, T. F., Pendergrass, A. G., Sanderson, B. M., Raible, C. C., and Smerdon, J. E.: Projected drought risk in 1.5°C and 2°C warmer climates. Geophys. Res. Lett., 44: 7419-7428, 2017.

Leimbach, M., Kriegler, E., Roming, N., and Schwanitz, J.: Future growth patterns of world regions-A GDP scenario approach. Glob. Environ. Change, 42:215-225, 2017.

Li, T., Guo, S., Liu, Z., Xiong, L., and Yin, J.: Bivariate design flood quantile selection using copulas. Hydrol. Res., 48(4):997-1013, 2016.

Li, W., Jiang, Z., Zhang, X., Li, L., & Sun, Y. Additional risk in extreme precipitation in China from 1.5 C to 2.0 C global warming levels. Science Bulletin, 63(4), 228-234, 2018.

Liu, K., & Jiang, D. Analysis of dryness/wetness over China using standardized precipitation evapotranspiration index based on two evapotranspiration algorithms. Chinese Journal of Atmospheric Sciences (in Chinese), 39(1), 23-36, 2015.

Liu, J., Wang, B., Cane, M. A., Yim, S. Y., and Lee, J. Y.: Divergent global precipitation changes induced by natural versus anthropogenic forcing. Nature, 493(7434), 656-659. https://doi.org/10.1038/nature11784, 2013.

Liu, W., Sun, F., Lim, W. H., Zhang, J., Wang, H., Shiogama, H., and Zhang, Y.: Global drought and severe drought-affected populations in 1.5 and 2 °C warmer worlds. Earth Syst. Dynam., 9:267-283, 2018a.

Liu, W., Lim, W. H., Sun, F., Mitchell, D., Wang, H., Chen, D., ... & Fischer, E. Global freshwater availability below normal conditions and population impact under 1.5 and 2 C stabilization

scenarios. Geophysical Research Letters, 45(18), 9803-9813, 2018b.
Liu, W., & Sun, F. Increased adversely-affected population from water shortage below normal conditions in China with anthropogenic warming. Science Bulletin, 64(9), 567-569, 2019.
Liu, X. F., Wang, S. X., Zhou, Y., Wang, F. T., Li, W. J., and Liu, W.L.: Regionalization and spatiotemporal variation of drought in china based on standardized precipitation evapotranspiration index (1961-2013). Adv. Meteorol., 18, 2015.
Lu, J., Vecchi, G. A., and Reichler, T.: Expansion of the Hadley cell under global warming. Geophys. Res. Lett., 34, L06805. https:// doi.org/10.1029/2006GL028443, 2007.
Mehran, A., AghaKouchak, A., and Phillips, T. J.: Evaluation of CMIP5 continental precipitation simulations relative to satellite- based gauge-adjusted observations, J. Geophys. Res.- Atmos., 119, 1695–1707, https://doi.org/10.1002/2013jd021152, 2014.
Mishra, A. K. and Singh, V. P.: A review of drought concepts. J. Hydrol., 391(1-2), 202-216, 2010.
Mitchell, D., James, R., Forster, P. M., Betts, R. A., Shiogama, H., and Allen, M.: Realizing the impacts of a 1.5 C warmer world. Nat. Climat. Change, 6(8), 735, 2016.
Muller, C. J., O'Gorman, P. A., and Back, L. E.: Intensification of precipitation extremes with warming in a cloud-resolving model. J. Clim., 24(11), 2784-2800, 2011.
Naumann, G., Alfieri, L., Wyser, K., Mentaschi, L., Betts, R. A., Carrao, H., and Feyen, L.: Global changes in drought conditions under different levels of warming. Geophys. Res. Lett., 45(7), 3285-3296, 2018.
O'Neill, B. C., Kriegler, E., Riahi, K., Ebi, K. L., Hallegatte, S., Carter, T. R., and van Vuuren, D. P.: A new scenario framework for climate change research: the concept of shared socioeconomic pathways. Climatic change, 122(3), 387-400, 2014.
Park, C. E., Jeong, S. J., Joshi, M., Osborn, T. J., Ho, C. H., Piao, S., and Kim, B. M.: Keeping global warming within 1.5° C constrains emergence of aridification. Nat. Clim. Change, 8(1), 70, 2018.
Peters, G. P.: The best available science to inform 1.5 C policy choices. Nat. Clim. Change, 6(7), 646. https://doi.org/10.1038/nclimate3000, 2016.
Roderick, M. L., Greve, P., & Farquhar, G. D. On the assessment of aridity with changes in atmospheric CO_2. Water Resources Research, 51(7), 5450-5463, 2015.
Routson, C. C., C. A. Woodhouse, J. T. Overpeck, J. L. Betancourt, J. L., and McKay, N.P.: Teleconnected ocean forcing of Western North American droughts and pluvials during the last millennium, Quat. Sci. Rev., 146, 238-250, 2016.
Salvadori, G., De Michele, C., and Durante, F. Multivariate design via copulas. Hydrol. Earth Syst. Sc. 8, 5523–5558, 2011.
Samir, K. C. and Lutz, W.: The human core of the shared socioeconomic pathways: Population scenarios by age, sex and level of education for all countries to 2100. Global Environmental Change, 42, 181-192, 2017.
Sanderson, B. M., Xu, Y., Tebaldi, C., et al.: Community climate simulations to assess avoided impacts in 1.5 and 2 °C futures. Earth Syst. Dynam., 8, 827-847, https://doi.org/10.5194/esd-8-827-2017, 2017.
Scheff, J. and Frierson, D. M.: Scaling potential evapotranspiration with greenhouse warming. J. Clim., 27(4), 1539-1558, 2014.
Schneider, D. P., & Reusch, D. B. Antarctic and Southern Ocean surface temperatures in CMIP5 models in the context of the surface energy budget. Journal of Climate, 29(5), 1689-1716, 2016.
Seager, R., Y. Kushnir, C. Herweijer, N. Naik, and J. Velez.: Modeling of tropical forcing of persistent droughts and pluvials over western North America: 1856–2000, J. Clim., 18, 4065-4088, doi:10.1175/JCLI3522.1, 2005.
Schilling, J., Freier, K.P., Hertig, E. and Scheffran, J.: Climate change, vulnerability and adaptation in North Africa with focus on Morocco. Agric. Ecosyst. Environ., 156, 12-26, 2012.
Smirnov, O., Zhang, M., Xiao, T., Orbell, J., Lobben, A., and Gordon, J.: The relative importance of climate change and population growth for exposure to future extreme droughts. Climatic Change, 138(1-2), 41-53, 2016.
Su, B., Huang, J., Fischer, T., Wang, Y., Kundzewicz, Z. W., Zhai, J., and Tao, H.: Drought losses in China might double between the 1.5° C and 2.0° C warming. P. Natl. Acad. Sci. USA., 115(42), 10600-10605, 2018.
Thober, S., Kumar, R., Wanders, N., Marx, A., Pan, M., Rakovec, O., ... & Zink, M. (2018). Multi-

model ensemble projections of European river floods and high flows at 1.5, 2, and 3 degrees global warming. Environmental Research Letters, 13(1), 014003.

Touma, D., Ashfaq, M., Nayak, M.A., Kao, S.-C., Diffenbaugh, N.S.: A multi-model and multi-index evaluation of drought characteristics in the 21st century. J. Hydrol., 526, 196–207. http://dx.doi.org/10.1016/j.jhydrol.2014.12.011, 2015.

Tsakiris, G., Kordalis, N., Tigkas, D., Tsakiris, V., and Vangelis, H.: Analysing drought severity and areal extent by 2D Archimedean copulas. Water Resour. Manage., 30, 1-13, 2016.

UNFCCC, 2015. Conference of the Parties. Adoption of the Paris Agreement, Paris. 1-32.

Vautard, R., Gobiet, A., Sobolowski, S., Kjellström, E., Stegehuis, A., Watkiss, P. and Jacob, D.: The European climate under a 2 C global warming. Environ. Res. Lett., 9(3), 034006, 2014.

Vicente-Serrano, S.M., Beguería, S., and López-Moreno, J.I.: A Multiscalar Drought Index Sensitive to Global Warming: The Standardized Precipitation Evapotranspiration Index. J. Clim., 23(7): 1696-1718. DOI:10.1175/2009jcli2909.1, 2010.

Wang, H. M., Chen, J., Cannon, A. J., Xu, C. Y. and Chen, H.: Transferability of climate simulation uncertainty to hydrological impacts. Hydrol. Earth Syst. Sc., 22(7), 3739-3759, 2018.

Wen, S. S., Wang, A. Q., Tao, H., Malik, K., Huang, J., Zhai, J., Jing, C., Rasul, G. and Su B.: Population exposed to drought under the 1.5 °C and 2.0 °C warming in the Indus River Basin. Atmos. Res., 218: 296-305, 2019.

Wong, G., Van Lanen, H.A.J. and Torfs, P.J.J.F.: Probabilistic analysis of hydrological drought characteristics using meteorological drought. Hydrol. Sci. J., 58 (2), 253-270, 2013.

Xie, S. P., Deser, C., Vecchi, G. A., Ma, J., Teng, H. and Wittenberg, A.: Global warming pattern formation: Sea surface temperature and rainfall. J. Climate, 23(4), 966–986. https://doi.org/10.1175/2009JCLI3329.1, 2010.

Xiao, M., Zhang, Q., Singh, V. P., & Chen, X. Probabilistic forecasting of seasonal drought behaviors in the Huai River basin, China. Theoretical and applied climatology, 128(3-4), 667-677, 2017.

Xu, K., Yang, D. W., Xu, X. Y., and Lei, H. M.: Copula based drought frequency analysis considering the spatio-temporal variability in Southwest China. J. Hydrol. 527, 630-640, 2015.

Yang, Y., Roderick, M. L., Zhang, S., McVicar, T. R., & Donohue, R. J. Hydrologic implications of vegetation response to elevated CO_2 in climate projections. Nature Climate Change, 9(1), 44, 2019.

Yin, J. B., Guo, S. L., He, S. K., Guo, J. L., Hong, X. J., and Liu, Z. J.: A copula-based analysis of projected climate changes to bivariate flood quantiles. J. Hydrol. 566, 23-42, 2018a.

Yin, J. B., Gentine, P., Zhou, S., Sullivan, C. S., Wang, R., Zhang, Y., and Guo, S.L.: Large increase in global storm runoff extremes driven by climate and anthropogenic changes. Nat. Commun. 9, 4389, 2018b.

Yin, J. B., Guo, S., Wu, X., Yang, G., Xiong, F., and Zhou, Y.: A meta-heuristic approach for multivariate design flood quantile estimation incorporating historical information. Hydrol. Res., 50(2), 526-544, 2019a.

Yin, J., Gentine, P., Guo, S., Zhou, S., Sullivan, S. C., Zhang, Y., ... & Liu, P. Reply to 'Increases in temperature do not translate to increased flooding'. Nature communications, 10(1), 1-5, 2019b.

Yevjevich, V. M.: Objective approach to definitions and investigations of continental hydrologic droughts, An. Hydrology papers (Colorado State University); 23., 1967.

Yu, M., Li, Q., Hayes, M. J., Svoboda, M. D., and Heim, R. R.: Are droughts becoming more frequent or severe in China based on the standardized precipitation evapotranspiration index: 1951-2010?. Int. J. Climatol.,34(3), 545-558, 2014.

Yuan, X., Zhang, M., Wang, L., & Zhou, T. Understanding and seasonal forecasting of hydrological drought in the Anthropocene. Hydrology and Earth System Sciences, 21(11), 5477-5492, 2017.

Zargar, A., Sadiq, R., Naser, B., and Khan, F. I.: A review of drought indices. Environ. Reviews, 19, 333-349, 2011.

Zhang, Q., Xiao, M.Z., and Singh, V.P.: Uncertainty evaluation of copula analysis of hydrological droughts in the East River basin, China. Global Planet., Change, 129, 1-9, 2015.

Zscheischler, J. and Seneviratne, S. I.: Dependence of drivers affects risks associated with compound events. Sci. Adv., 3(6), e1700263, 2017.

1

List of Tables

Table 1 Information about the 13 GCMs used in this study

No.	Model name	Resolution	Institution
1	BNU-ESM	2.8 × 2.8	Collegeof Global Change and Earth System Science, Beijing Normal University
2	CanESM2	2.8 × 2.8	Canadian Centre for Climate Modelling and Analysis
3	CNRM-CM5	1.4 × 1.4	Centre National de Recherches Météorologiques and Centre Européen de Recherche et Formation Avancée en Calcul Scientifique
4	CSIRO-Mk3.6.0	1.8 ×1.8	Commonwealth Scientific and Industrial Research Organization and Queensland Climate Change Centre of Excellence
5	GFDL-CM3	2.5 × 2.0	NOAA Geophysical Fluid Dynamics Laboratory
6	GFDL-ESM2G	2.5 × 2.0	
7	GFDL-ESM2M	2.5 × 2.0	
8	IPSL-CM5A-LR	3.75 × 1.9	Institut Pierre Simon Laplace
9	IPSL-CM5A-MR	2.5 × 1.25	
10	MIROC-ESM-CHEM	2.8 × 2.8	Japan Agency for Marine-Earth Science and Technology, Atmosphere and Ocean Research Institute (The University of Tokyo), and National Institute for Environmental Studies
11	MIROC-ESM	2.8 × 2.8	
12	MIROC5	1.4 × 1.4	Atmosphere and Ocean Research Institute (The University of Tokyo), National Institute for Environmental Studies, and Japan Agency for Marine-Earth Science and Technology
13	MRI-CGCM3	1.1 × 1.1	Meteorological Research Institute

Table 2 Drought Categories in the SPEI

SPEI	Categories
>-0.5	Near Normal
-1.0 to -0.5	Mild drought
-2.0 to -1.0	Moderate drought
<-2.0	Extreme~~ly~~ drought

Table 3 Global population and GDP at the 1.5℃ and 2.0℃ warming climates

	SSP126	SSP124	SSP585
1.5°C-population (million)	1516.9	1553.5	1510.8
2.0°C-population (million)	1666.7	1731.2	1603.1
1.5°C-GDP (billion USD)	35875.0	34244.0	35668.5
2.0°C-GDP (billion USD)	116991.1	56271.6	58916.2

带格式的：正文

List of Figures

Fig. 15. Projected changes in joint 50-year return periods of droughts when using the -0.5 as the threshold and the -0.8 as the threshold between the 1.5°C and 2.0°C warming target

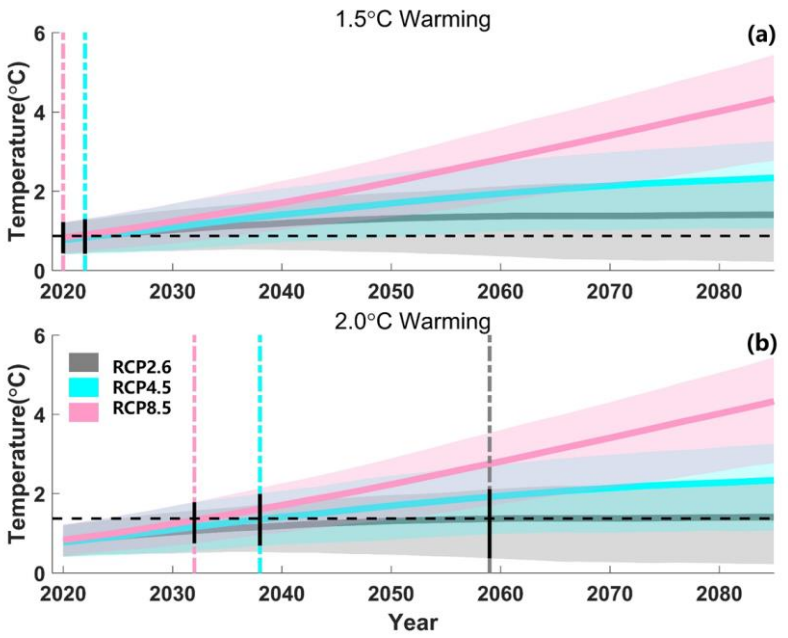

Fig. 1. Projected global mean temperatures when reaching 1.5°C warming (a**) and 2.0°C warming (**b**).**

Development of centered 30-year global average temperatures for all 13 General Circulation Models (GCMs) and 3 Representative Concentration Pathways (RCPs) included in this study. The vertical dark lines mark the uncertainty when the warming target is reached. In **Fig.1a**, the determined time in RCP2.6 is the same with that in RCP4.5, so the vertical dashed grey line is covered by the dashed cyan line.

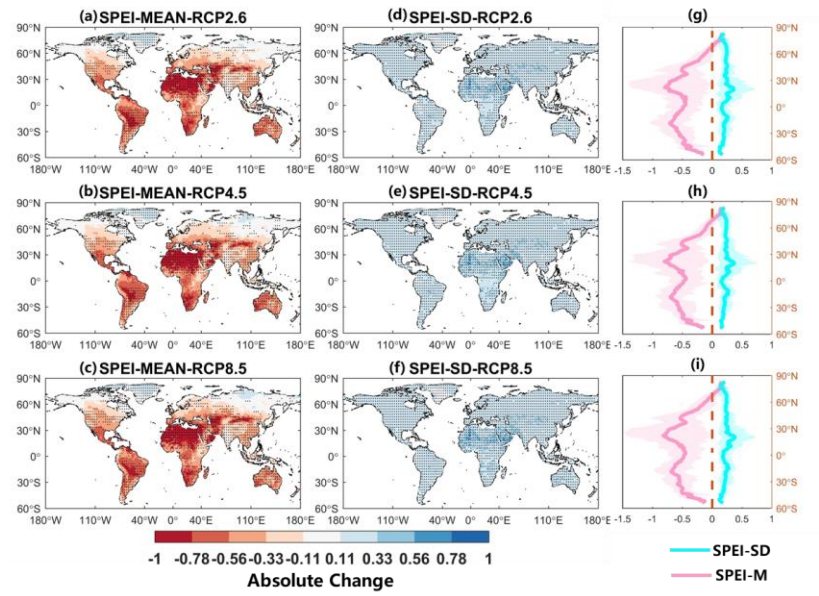

Fig. 2. Projected changes in the mean and standard deviation of SPEI under the 1.5°C warming target

Maps of the projected changes in the mean (**a,c,e**) and standard deviation (**b,d,f**) of SPEI from historical reference period (1976-2005) to the 1.5°C warming target under RCP2.6, RCP4.5, and RCP8.5. (**g,h,i**) Zonal results for changes in 1° latitude bin. The stippling (**a-f)** is shaded for areas where at least 80% (i.e., 10 out of 13) of the GCMs agree on the sign of the change.

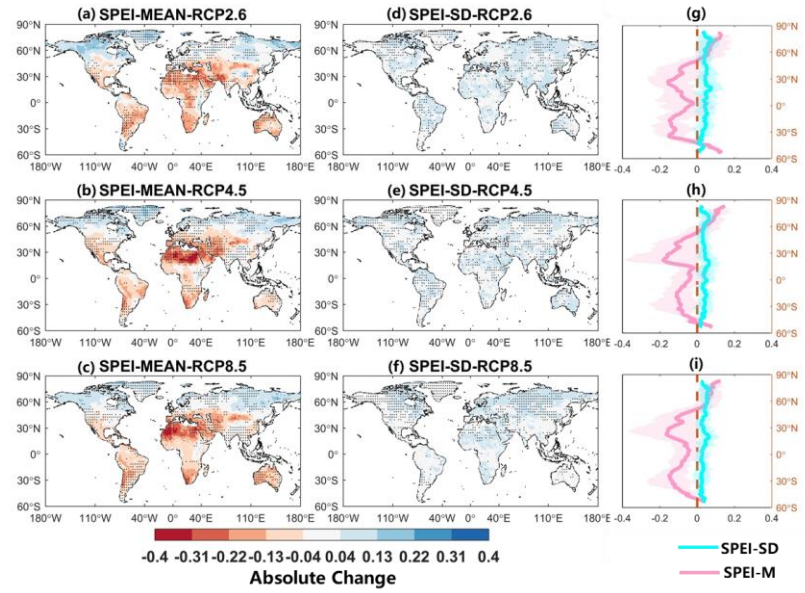

Fig. 3. Projected changes in the mean and standard deviation of SPEI between the 1.5°C and 2.0°C warming target

Maps of the projected changes in the mean (**a,c,e**) and standard deviation (**b,d,f**) of SPEI from 1.5°C to the 2.0°C warming target under RCP2.6, RCP4.5, and RCP8.5. (**g,h,i**) Zonal results for changes in 1° latitude bin. The stippling (**a-f)** is shaded for areas where at least 80% (i.e., 10 out of 13) of the GCMs agree on the sign of the change.

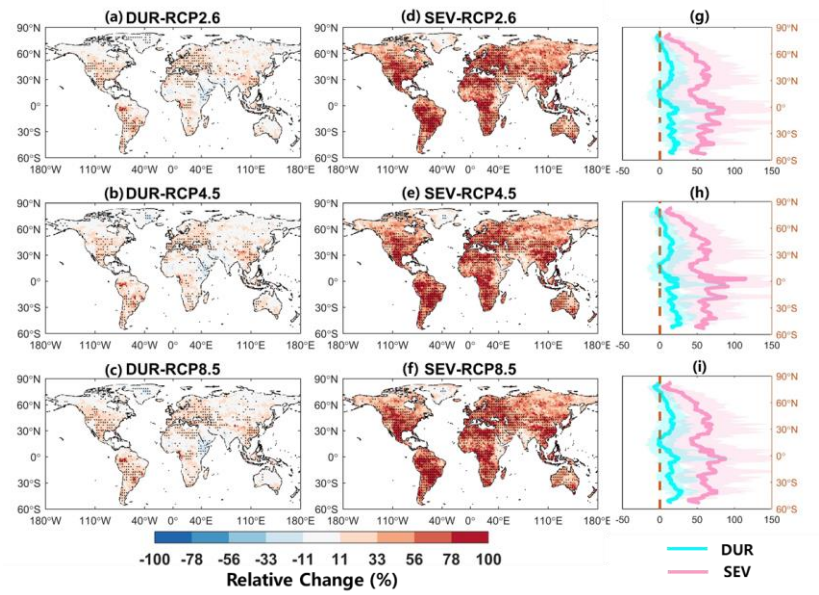

Fig. 4. Projected changes in drought duration and severity under the 1.5°C warming target

Maps of the relative changes (%) in the multi-model ensemble mean drought duration (**a,c,e**) and drought severity (**b,d,f**) from the reference period (1976-2005) to the 1.5°C warming target under RCP2.6, RCP4.5, and RCP8.5. (**g,h,i**) Zonal results for drought duration and severity in 1° latitude bin. The stippling (**a-f)** is shaded for areas where at least 80% (i.e., 10 out of 13) of the GCMs agree on the sign of the change.

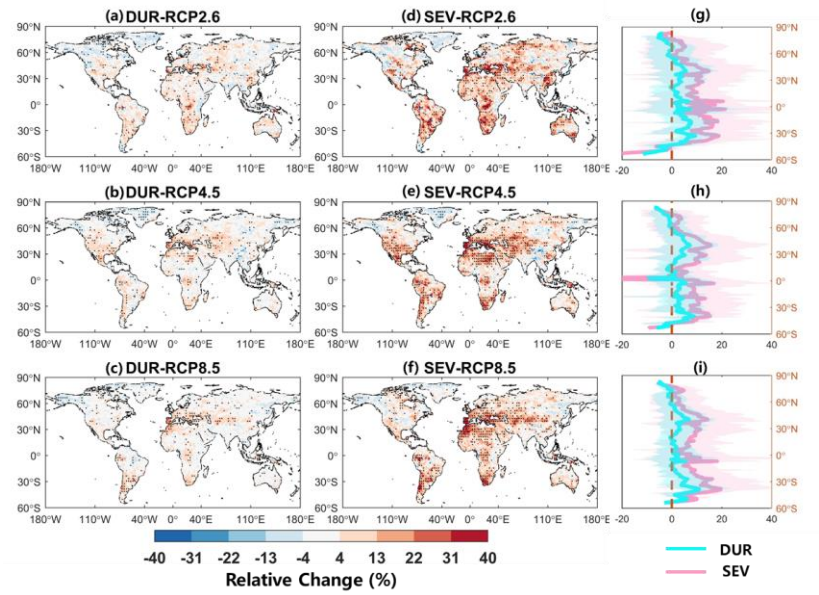

Fig. 5. Projected changes in drought duration and severity between the 1.5°C and 2.0°C warming target

Maps of the relative changes (%) in the multi-model ensemble mean drought duration (**a,c,e**) and drought severity (**b,d,f**) from the 1.5°C to the 2.0°C warming target under RCP2.6, RCP4.5, and RCP8.5. (**g,h,i**) Zonal results for drought duration and severity in 1° latitude bin. The stippling (**a-f)** is shaded for areas where at least 80% (i.e., 10 out of 13) of the GCMs agree on the sign of the change.

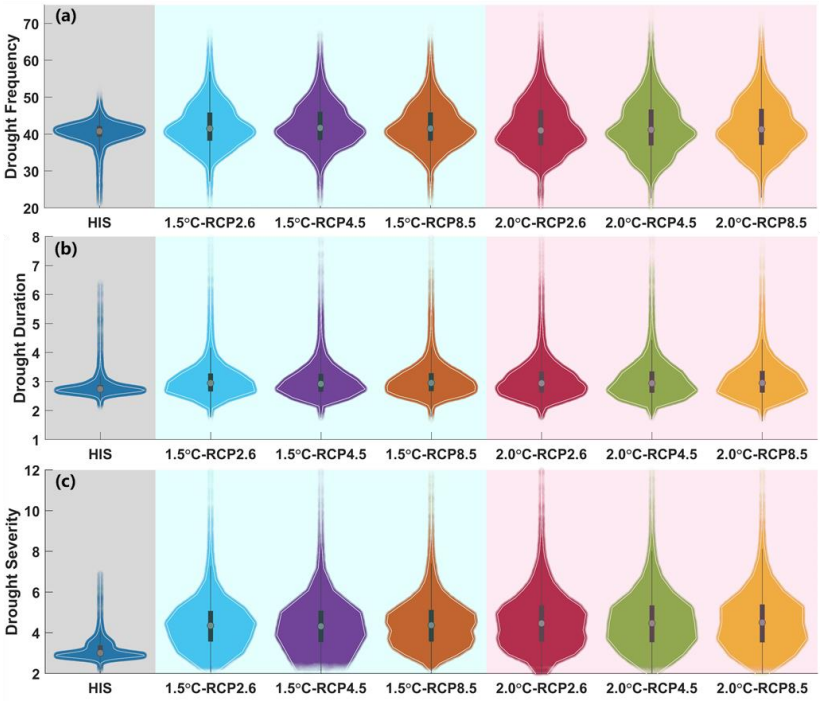

Fig. 6. Distributions for drought characteristics under different time periods

Distributions in the multi-model ensemble mean drought frequency (**a**), drought duration (**b**) in months, and drought severity (**c**) across global land areas for the reference period (1976-2005), the 1.5°C, and the 2.0°C warming target, respectively.

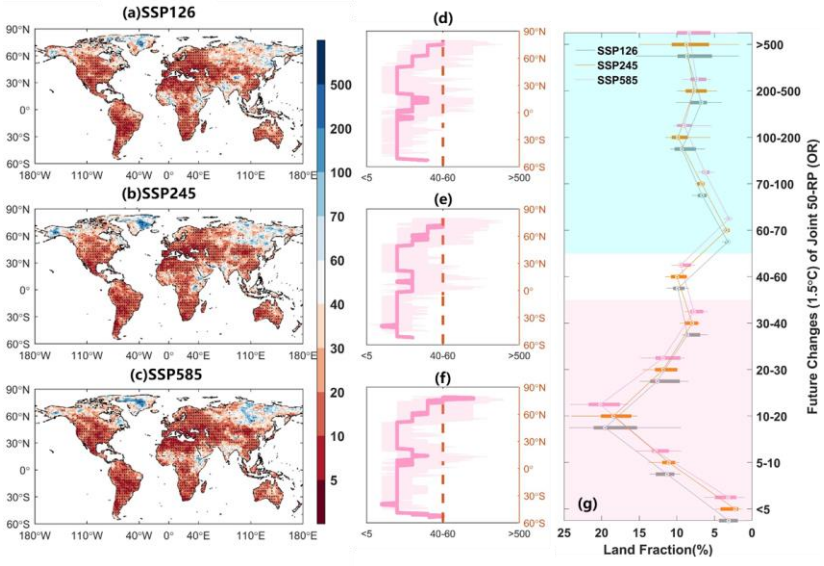

Fig. 7. Projected changes in joint 50-year return periods of droughts under the 1.5°C warming target

Projected GCMs median changes in joint 50-year return periods of droughts (duration and severity) from the reference period to the 1.5°C warming target under SSP126, SSP245, and SSP585~~RCP2.6, RCP4.5, and RCP8.5~~. **(d,e,f)** Zonal results in each 1° latitude bin; **(g)** Global land fraction subject to drought risk changes of different magnitudes under three scenarios. For an individual climate model output, the land fraction is calculated by using the ratio of grid counts located at certain extent (e.g., <5) divided by the world land grid counts (excluding Antarctic). Each box is stemmed from the 13 climate models results and the circle in each box represents the multi-model ensemble median results.~~Global land fraction for each change category~~. The stippling (**a-c**) is shaded for areas where at least 80% (i.e., 10 out of 13) of the GCMs agree on the sign of the change.

带格式的：字体颜色：蓝色

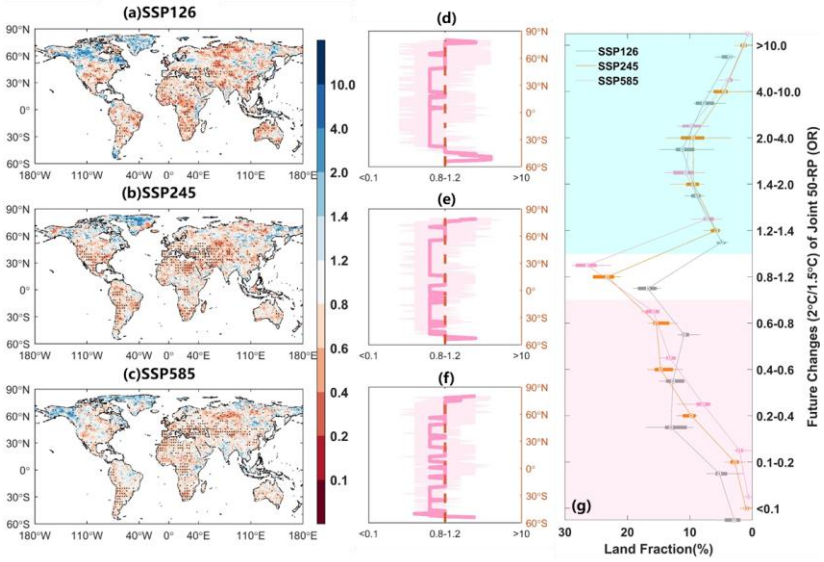

Fig. 8. Projected changes in joint 50-year return periods of droughts between the 1.5°C and 2.0°C warming target

Projected GCMs median changes in joint 50-year return periods of droughts (duration and severity) from the 1.5°C to the 2.0°C warming target under SSP126, SSP245, and SSP585~~RCP2.6, RCP4.5, and RCP8.5~~. **(d,e,f)** Zonal results in each 1° latitude bin; **(g)** Global land fraction subject to drought risk changes of different magnitudes under three scenarios. For an individual climate model output, the land fraction is calculated by using the ratio of grid counts located at certain extent (e.g., <5) divided by the world land grid counts (excluding Antarctic). Each box is stemmed from the 13 climate models results and the circle in each box represents the multi-model ensemble median results.~~Global land fraction for each change category.~~ The stippling (**a-c)** is shaded for areas where at least 80% (i.e., 10 out of 13) of the GCMs agree on the sign of the change.

带格式的：字体颜色：蓝色

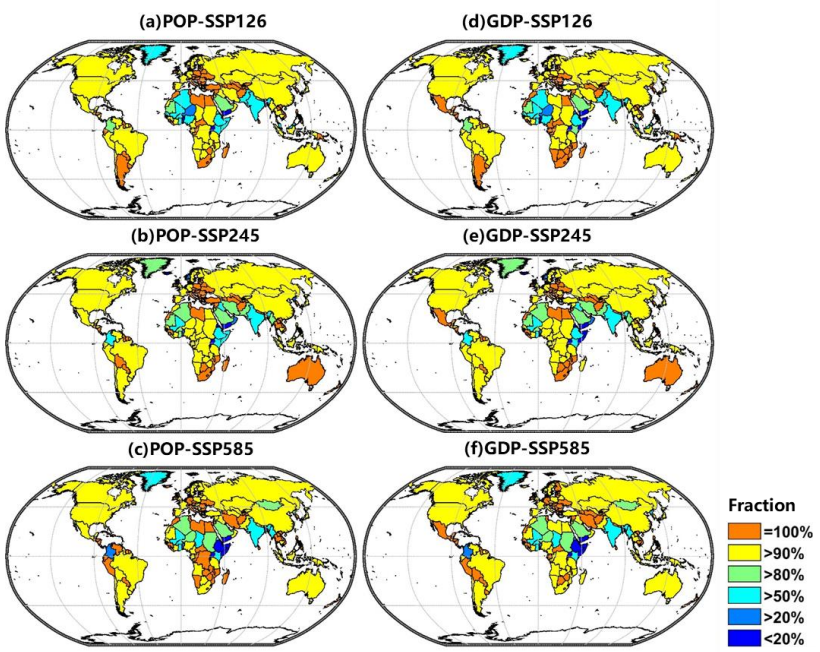

Fig. 9. National population and GDP fraction exposing to more frequent severe droughts under the 1.5°C warming target

Maps of the population (**a,c,e**) and Gross Domestic Product (GDP) (**b,d,f**) fractions that exposed to increasing drought risks from the reference period to the 1.5°C warming target under SSP126, SSP245, and SSP585~~RCP2.6, RCP4.5, and RCP8.5~~ scenarios. The color-bar in the right side represents six ranks of the population and GDP fractions.

带格式的：字体颜色：蓝色

带格式的：字体颜色：蓝色

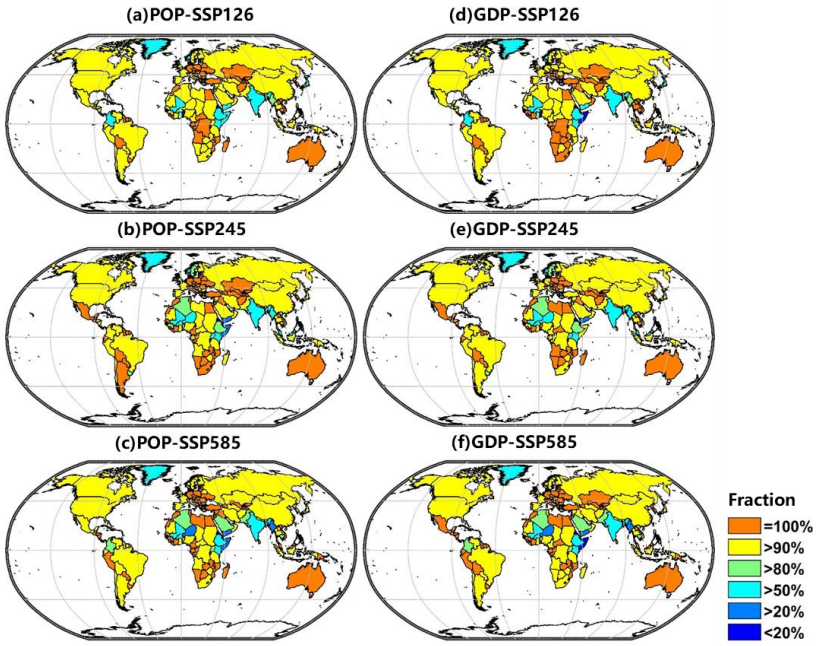

Fig. 10. National population and GDP fraction exposing to more frequent severe droughts under the 2.0°C warming target

Maps of the population (**a,c,e**) and Gross Domestic Product (GDP) (**b,d,f**) fractions that exposed to increasing drought risks from the reference period to the 2.0°C warming target under ~~RCP2.6~~SSP126, SSP245~~RCP4.5~~, and SSP585~~RCP8.5~~ scenarios. The color-bar in the right side represents six ranks of the population and GDP fractions.

带格式的：字体颜色：蓝色

带格式的：字体颜色：蓝色

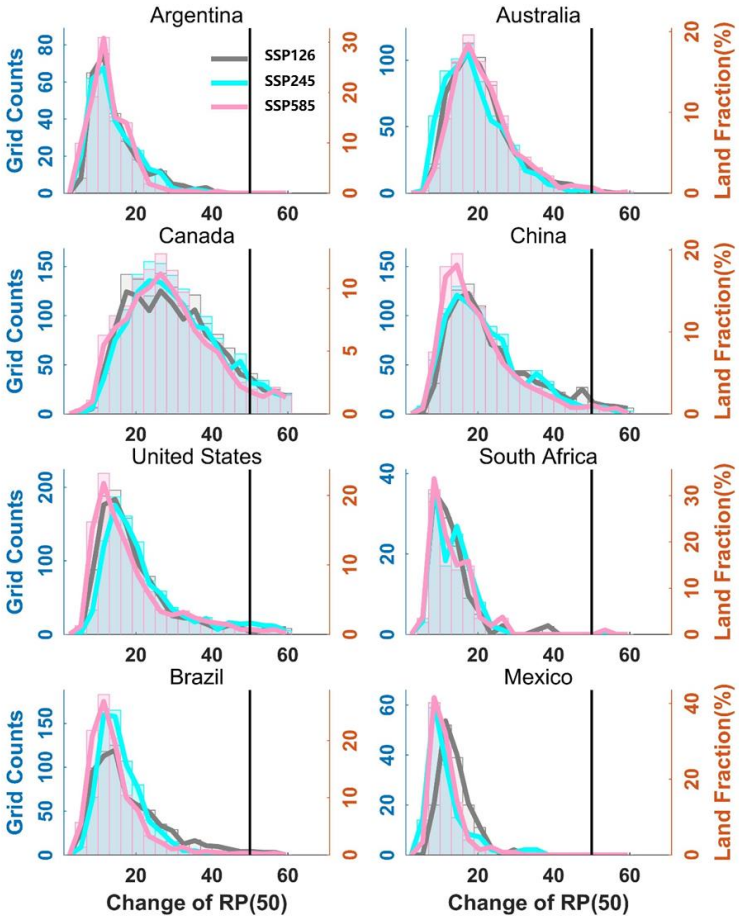

Fig. 11. Projected changes of drought risks for 8 typical drought-prone countries under the 1.5°C warming target

Projected GCMs median changes in joint 50-year return periods of droughts (duration and severity) as a function of land fraction for 8 typical drought-prone countries from the reference period to the 1.5°C warming target under RCP2.6, RCP4.5, and RCP8.5.

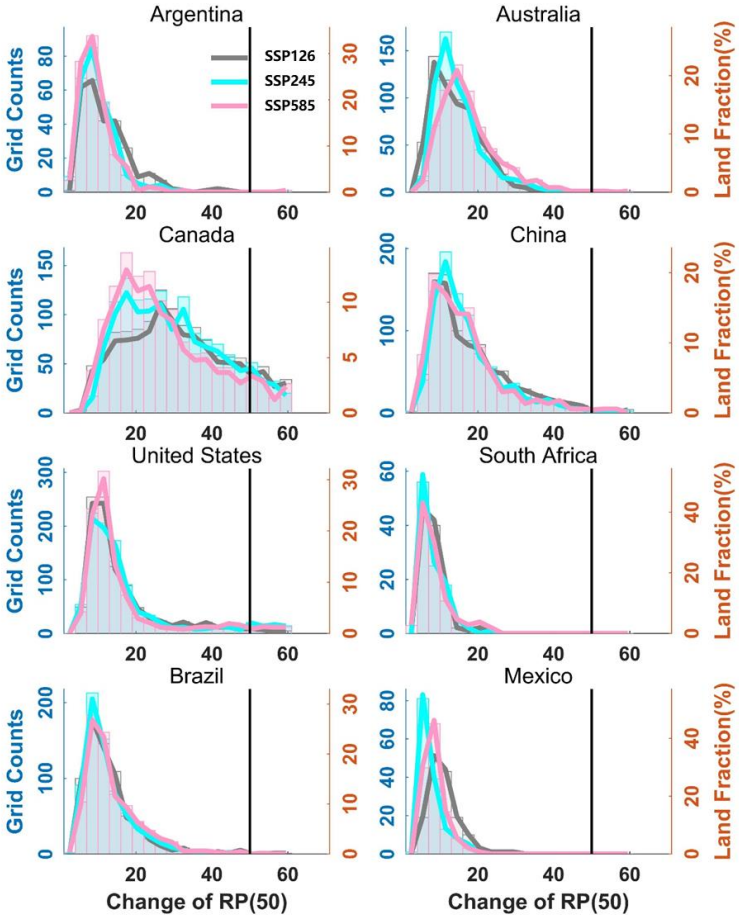

Fig. 12. Projected changes of drought risks for 8 typical drought-prone countries under the 2.0 °C warming target

Projected GCMs median changes in joint 50-year return periods of droughts (duration and severity) as a function of land fraction for 8 typical drought-prone countries from the reference period to the 2.0°C warming target under RCP2.6, RCP4.5, and RCP8.5.

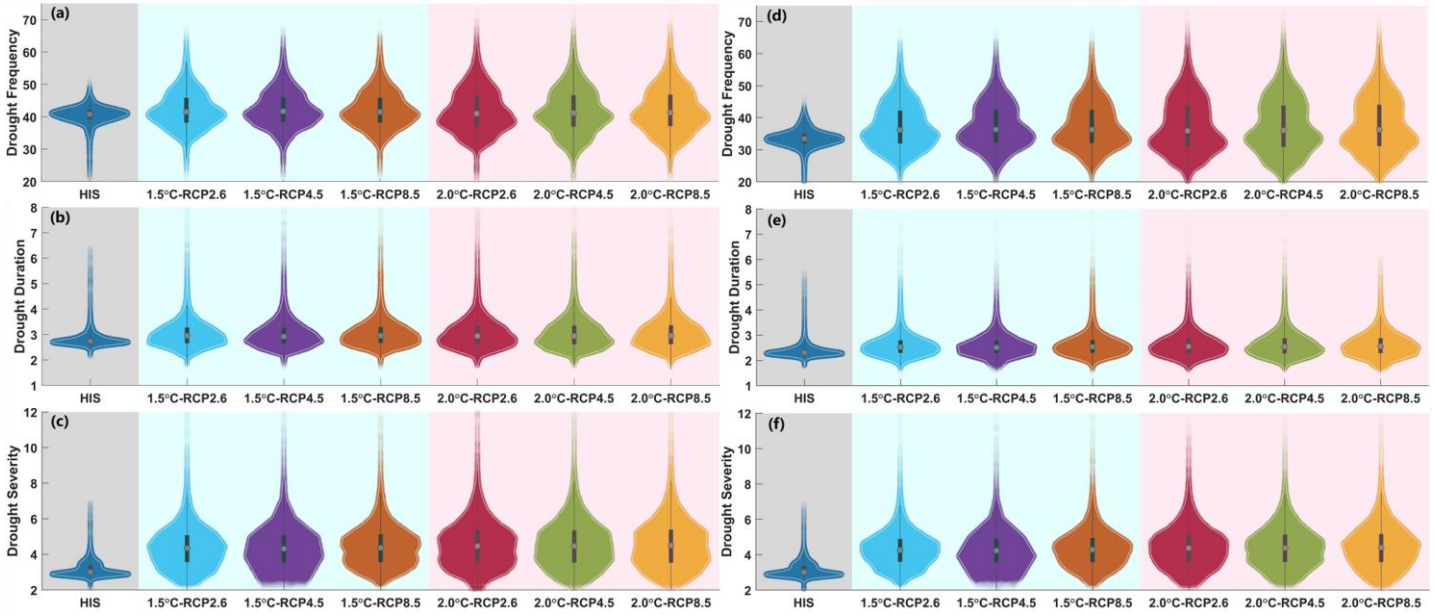

Fig. 13. Distribution for drought characteristics when using the -0.5 **as the threshold (a,b,c) and the** -0.8 **as the threshold (d,e,f), respectively.**

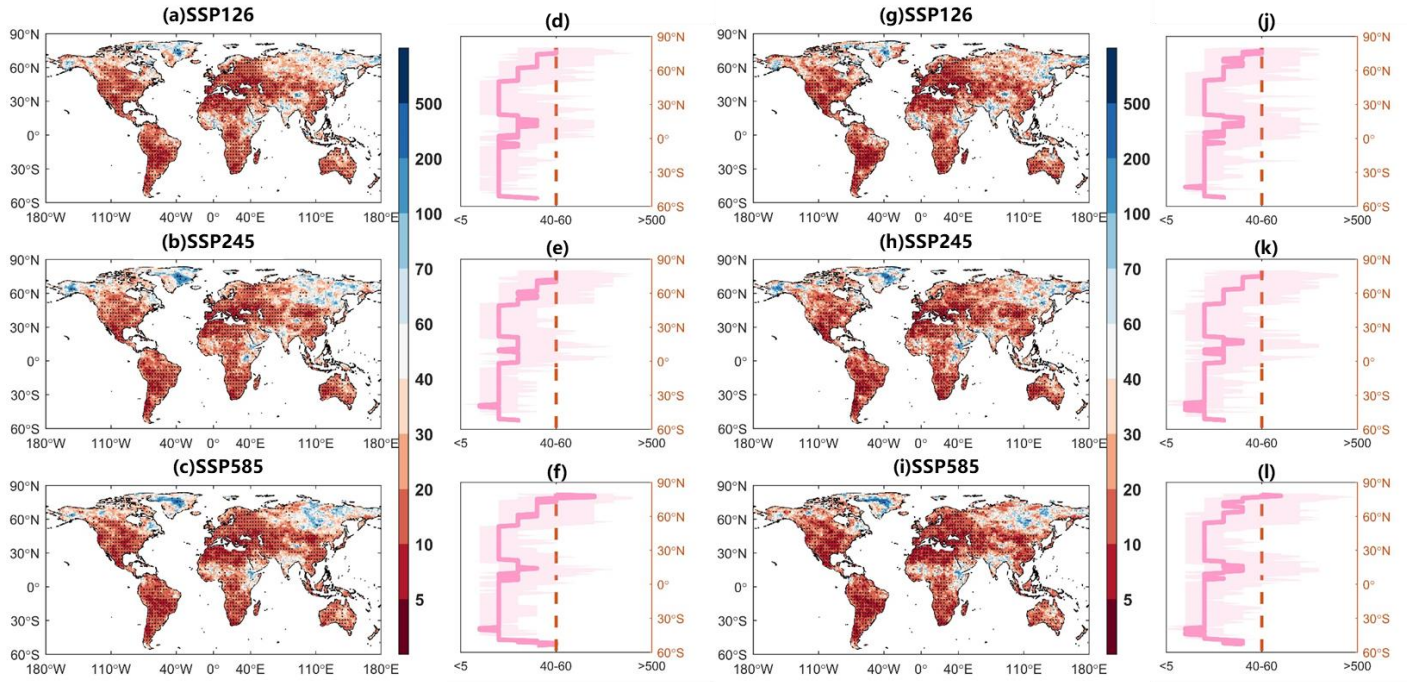

158

159 **Fig. 14 Projected changes in joint 50-year return periods of droughts when using the -0.5 as the threshold (a-f) and the -0.8 as the threshold (g-l) under**

160 **the 1.5°C warming target**

带格式的：字体颜色：蓝色

带格式的：字体：非加粗，字体颜色：蓝色

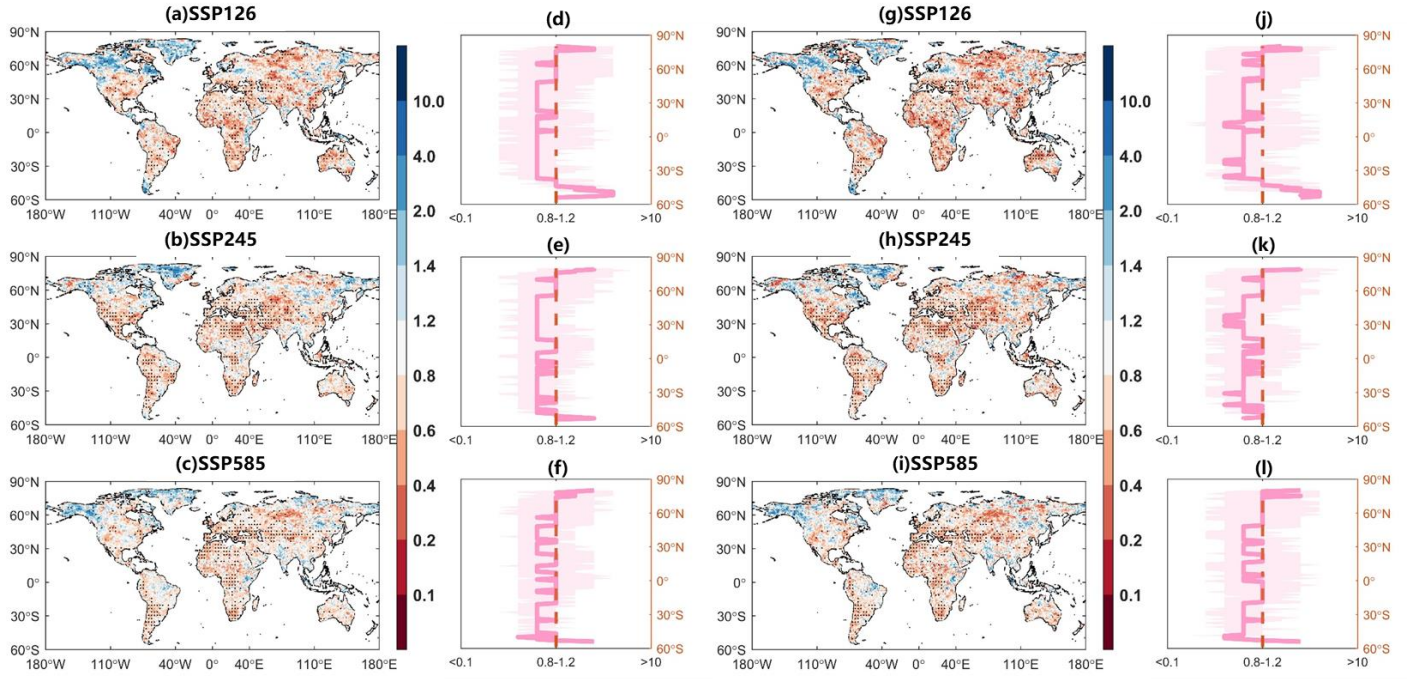

161

162 **Fig. 15 Projected changes in joint 50-year return periods of droughts when using the -0.5 as the threshold (a-f) and the -0.8 as the threshold (g-l)**

163 **between the 1.5°C and 2.0°C warming target**

164

带格式的：字体颜色：蓝色

带格式的：字体：非加粗，字体颜色：蓝色